METABOLIC PROFILING OF CHONDROCYTE MECHANOTRANSDUCTION UNDER PHYSIOLOGICAL AND INJURIOUS MECHANICAL STIMULATION

by

Aidan John Gregory

A thesis submitted in partial fulfillment
of the requirements for the degree

of

Master of Science

in

Mechanical Engineering

MONTANA STATE UNIVERSITY
Bozeman, Montana

December 2025

TABLE OF CONTENTS

LIST OF TABLES

Table Page

LIST OF FIGURES

Figure Page

ABSTRACT

Osteoarthritis (OA) is the leading cause of disability worldwide, affecting over 600 million people. OA is characterized by the progressive degradation of articular cartilage, subchondral bone, and synovium. In 2016, OA was responsible for an estimated $80 billion in healthcare spending in the USA, and the population of patients with doctor-diagnosed OA is expected to reach 1 billion by 2050 [1]. OA progression is increasingly recognized as both a mechanically driven and metabolically regulated disease. Altered cellular responses to load interact with dysregulated metabolic pathways, causing OA progression and an imbalance of matrix synthesis and degradation. Cartilage injury is a major clinical concern because it initiates the onset of post-traumatic Osteoarthritis (PTOA), leading to progressive pain, joint dysfunction, and long-term disability.

In summary, the overall goal of this research is to better inform future studies on the role of central metabolism in chondrocyte mechanotransduction. Specifically, the role of physiological and injurious mechanical stimulation on the metabolic profiles of chondrocytes will be examined. By integrating *in vitro* mechanical testing with targeted metabolomics, this work aims to identify how different mechanical stimuli affect central metabolism in human OA and normal bovine chondrocytes.

.

INTRODUCTION

1.0 INTRODUCTION

Background

Osteoarthritis (OA) is the leading cause of disability worldwide, affecting over 600 million people worldwide. OA is characterized by the progressive degradation of articular cartilage, subchondral bone, and synovium [2]. In 2016, OA was responsible for an estimated $80 billion in healthcare spending in the USA. The prevalence and economic burden of OA are expected to rise substantially in the next three decades, driven largely by demographic shifts and increasing obesity. The population of patients with doctor-diagnosed OA is expected to reach 1 billion by 2050 [1]. OA most commonly affects the knees and hips, causing joint swelling, pain, and lack of mobility in the joint. Knee osteoarthritis (KOA) is the most extensively studied form of OA due to its accessibility and significant impact [3]. For the purposes of this work, references to OA will specifically pertain to KOA unless otherwise noted. While current interventions can provide symptomatic relief, there are presently no FDA-approved disease modifying therapies for OA; available treatment options are limited to pain management or, in advanced cases, partial/total joint replacement [3].

Previous studies defined macroscopic tissue changes, joint destabilization, immune responses, and “erosion” as key pathological features of OA progression. However, the underlying intracellular metabolic response remains poorly understood [4]. Therefore, to better distinguish the exact mechanism of OA progression, we must look at the individual metabolic states of healthy and diseased articular cartilage.

Structure of Cartilage

Articular cartilage is a specialized connective tissue that provides a smooth, low-friction surface for joint articulation and transduces mechanical loads through the joint. Articular cartilage exists in a state of hypoxia, with no blood vessels or nerves. As a type of hyaline cartilage, it typically ranges from 2-4mm in thickness. It is composed of a dense extracellular matrix (ECM) with a sparse distribution of chondrocytes. The ECM is primarily composed of water, collagen, and proteoglycans. This composition supports the mechanical function of articular cartilage, by maintaining internal pressurization under load. Articular cartilage has 4 zones: the superficial zone, the middle zone, the deep zone, and the calcified zone.

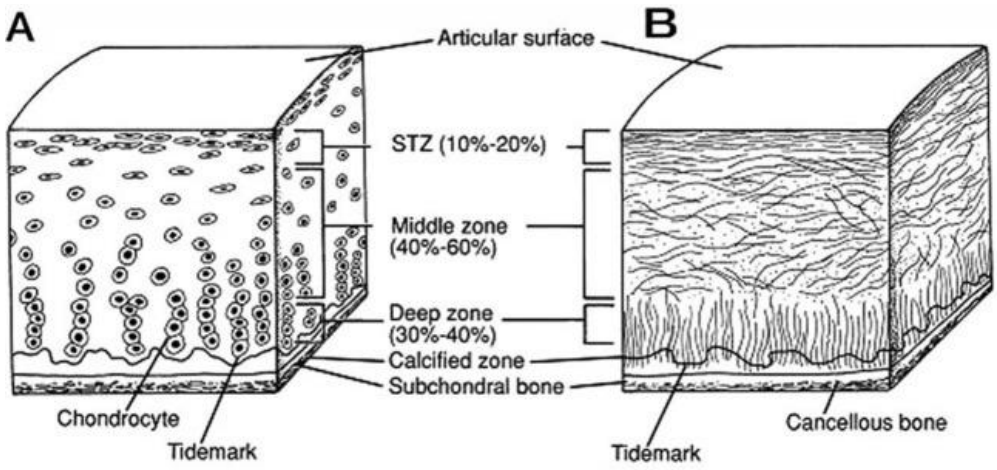

Figure 1: Articular cartilage Cross Section, A: Chondrocyte Density, Shape and Orientation, B: Collagen Fibral Density and Orientation [5].

The superficial zone represents approximately 10-20% of articular cartilage thickness. With collagen (primarily type II and IX) and chondrocytes oriented longitudinally (parallel to the cartilage surface), the primary functions of the superficial zone are to secrete lubricants such as superficial zone protein and protect the deeper layers from shear stresses. Chondrocytes in the superficial zone secrete proteins that function in the boundary layer, helping with lubrication of

the joint [6]. The superficial zone is in contact with synovial fluid. The middle zone (directly below the superficial zone) represents approximately 40-60% of cartilage thickness. In this zone, chondrocytes and collagen are organized indirectly and the primary function is to resist compressive forces. The deep zone makes up approximately 30% of articular cartilage thickness. It provides the greatest resistance to compressive forces. Deep zone collagen is organized axially (perpendicular to the cartilage surface). The deep zone has the highest content of proteoglycans, largest diameter of collagen fibrils, and lowest water concentration. All these contribute to the structural rigidity of the deep zone and the overall stiffness of articular cartilage. The calcified zone is defined by a tide mark and secures the cartilage to the bone. Here chondrocytes are sparce. While the zonal architecture of articular cartilage defines its mechanical gradients the ECM and PCM (pericellular matrix) play central roles in mediating these functional properties.

Extracellular Matrix/Pericellular Matrix

The ECM is a highly specialized, dynamic network of macromolecules that provides both structural support and transmission of biomechanical cues to chondrocytes. The ECM is primarily made up of water, approximately 65-80% by weight. There are two major load bearing macromolecules: collagen (mainly type II), and proteoglycans (mainly aggrecan).
Collagen is the most abundant structural component of the cartilage ECM and makes up 60% of the dry weight. Type II collagen is estimated to make up 90-95% of the total collagen in the ECM. All types of collagens contain a specific region that is composed of 3 polypeptide chains wound into a triple helix. The triple helix structure provides tensile and shear properties important for maintaining the stability of the matrix [7].

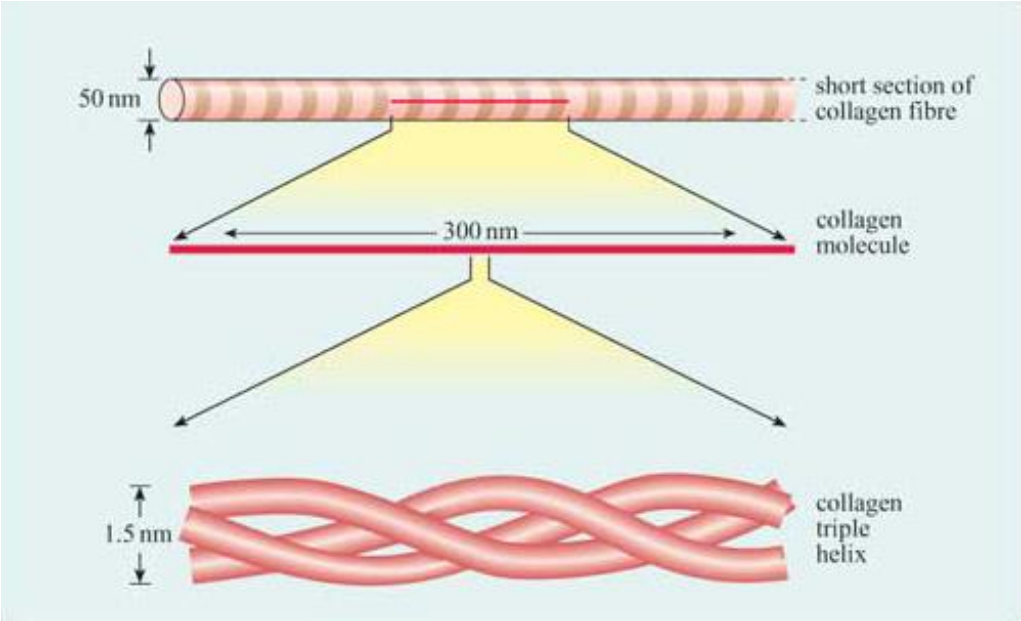

Figure 2: Collagen Type II, Structure Showing triple helix [8].

Aggrecan is the largest and most abundant proteoglycan in the ECM both by size and molecular weight. It interacts with hyaluronan to form extensive proteoglycan aggregates that occupy interfibrillar spaces throughout cartilage. These aggregates are essential for maintaining osmotic pressure, which enables cartilage to resist compressive loads, preserve its structural integrity, and protect chondrocytes.

The PCM is a specialized microenvironment that surrounds each chondrocyte and plays a critical role in regulating mechanotransduction within articular cartilage. This narrow region, approximately 2-3um thick, lies in-between the chondrocyte and the surrounding ECM [9]. The PCM is highly sensitive to changes in chondrocyte metabolism and serves as a key site for matrix turnover [10]. Notably, aggrecan, one of the primary proteoglycans in cartilage, undergoes the fastest turnover in the PCM, and the majority of newly synthesized aggrecan is localized in the PCM [11]. Aggrecan is among the first matrix components to degrade during the onset and progression of OA, underscoring its structural and biomechanical significance. These

characteristics position the PCM as a potential critical contributor to the early pathogenesis of OA.

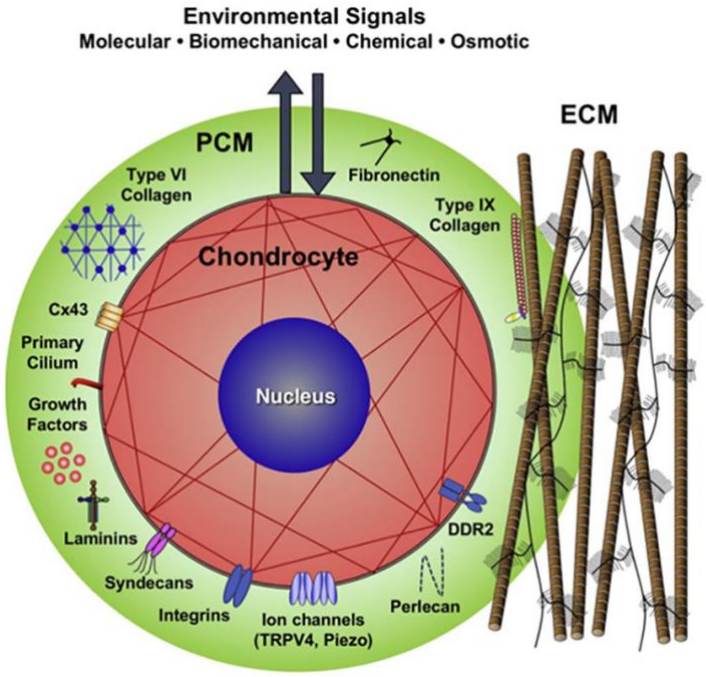

Figure 3: Chondrocyte, PCM, and ECM Diagram [12].

At the center of cartilage function and maintenance are chondrocytes. The sole resident cells of articular cartilage, which orchestrate matrix synthesis, turnover, and response to mechanical stimuli. Chondrocytes are highly differentiated cells, after growth, there is no evidence of cell division, indicated that they are long living [13]. This slow or absence of proliferation makes it difficult for cartilage to heal once the onset of OA takes place. *In vivo* chondrocytes are "attached" to the PCM and dependent on this connection to sense mechanical stimulation. Therefore, to provide a three dimensional environment when studying chondrocytes *in vitro* we must use a similar mechanical construct, like agarose.

Mechanotransduction and Metabolomics

OA progression is increasingly recognized as a mechanically driven and metabolically regulated disease. Altered cellular responses to load interact with dysregulated metabolic pathways, causing OA progression and an imbalance of matrix synthesis and degradation. Mechanical stimulation and chemical cues influence chondrocytes metabolism. Emerging data link bioenergetic stress and metabolite imbalance to the inability of chondrocytes to maintain homeostasis [14, 15].

Chondrocytes transduce mechanical signals into biochemical responses through many mechanisms including a complex network of ion channels and signaling cascades. Chondrocytes react to PCM deformation by activating a series of extracellular ion channels. Most notably calcium channels, where changes in Ca^{2+} concentration are among the most fundamental chondrocyte response to mechanical stimulation. When chondrocytes are healthy and joint mechanics are intact, these channels produce the proper amount of Ca^{2+} to maintain homeostasis in the tissue. However, if the cells are diseased, or joint mechanics are not functioning properly, chondrocytes will shift to catabolic processes that will deteriorate the matrices within the tissue [16]. Piezo 1 and 2 are the most studied calcium ion channels and can trigger signaling cascaded when activated. In mesenchymal stem cells, which are precursors to articular chondrocytes, the activation of Piezo 1 via hydrostatic pressure can activate proteins that affect the phenotype of the surrounding matrix [17]. When the surrounding phenotype changes, the inputs (via hydrostatic pressure, or mechanical loading) change to further alter the activation of ion channels, causing a signal cascading effect.

Mechanical stimulation directly modulates chondrocyte metabolism, shifting the balance between anabolic energy generation and catabolic stress response. In consistent, physiological

stimulation in healthy joints, ATP production and glycolysis is promoted [18]. Under abnormal, excessive loading, or injury conditions, a stress and inflammatory response is seen. Mitochondrial dysfunction and lactate accumulation have been seen as responses to abnormal loading conditions [19]. Recent studies demonstrated altered amino acid metabolism, lipid utilization, and redox imbalance in OA samples [20].

Metabolomics is the study of small molecules, or metabolites, within a biological system such as a cell or tissue. Metabolites are the end-product or intermediates of cellular metabolism and play an essential role in supporting biosynthesis and energy producing pathways. Many are precursors to proteins, amino acids, lipids, and nucleotides, which in turn contribute to ECM formation in cartilage. Unlike genomic or transcriptomic approaches that measure potential activation through gene expression or RNA sequencing, metabolomics provides a direct snapshot of the current state of metabolism of chondrocytes. This allows a direct functional readout of the cell's physiological status, reflecting how chondrocytes are responding to their microenvironment at any given time [21].

Metabolomics uses a variety of specialized equipment and advanced multivariate data analysis. The main tool is mass spectrometry (MS) which is one of the most widely used approaches for metabolomic profiling. It allows for large scale quantitative analysis of metabolites and offers a range of sensitivity and specificity, making it a useful tool for research. In metabolomics, MS is typically coupled with a chromatographic separation method, most often liquid chromatography (LC). LC reduces ion suppression and increases resolution between compounds of similar mass-to-charge ratios. The MS machine used for this dissertation is a Waters Synapt quadrupole time-of-flight (Waters, Milford, Massachusetts).

In basic principles, MS has three main stages: ionization, mass analysis, and detection. First, a voltage is applied to the liquid sample, this created a spray of charged droplets that evaporate to charged ions. Either positive or negative ionization modes may be used depending on the chemical properties of the metabolites of interest.

Once ionized, the metabolites are introduced into the mass analyzer where they are separated based on their mass-to-charge ratio (m/z score). Typically, most metabolites form singly charged ions under electrospray conditions, so their m/z score corresponds directly to the molecular weight of the compound. Some metabolites carry multiple charges, and the overall m/z value is the molecular weight divided by the number of charges. This principle allows the mass analyzer to detect different metabolites with high precision and accuracy.

Finally, the separated ions are detected and converted into electronic signals proportional to abundance. The resulting abundance of metabolites can be used to calculate absolute abundances through the use of calibration curves made from known concentrations of internal metabolite standards. Alternatively, relative abundance can be used as a quantitative measure. Together, the stages of ionization, mass analysis and detection form the basis of MS and enable quantification of metabolites within complex biological samples [22, 23].

Role of Injury

Cartilage injury is a major clinical concern because it initiates the onset of post-traumatic Osteoarthritis (PTOA), leading to progressive pain, joint dysfunction, and long-term disability. Epidemiological studies show that individuals with a history of knee injuries are 3 to 6 times more likely to develop knee OA compared to those without such injury [24]. Following joint injury proinflammatory mediators are produced and matrix degradation begins. Matrix

degradation results in abnormal loading for chondrocytes. Chondrocytes, being mechanosensitive, respond differently to abnormal loading conditions than in a healthy joint. When the degradation of the ECM exceeds the rate of remodeling, OA occurs. For most patients OA has multiple risk factors. Sex, BMI, genetics, age, and joint trauma are among the top risk factors for OA. For the purposes of this thesis, joint trauma and abnormal loading conditions will be the primary focus, as these factors directly affect the progression of PTOA [25].

Experimental models of PTOA typically rely on controlled joint injuries, such as anterior cruciate ligament (ACL) transection, meniscal destabilization, or mechanical impact loading. Surgical ACL transection, typically done in mice or rabbits, produces rapid and reproducible joint instability that mimics the onset of PTOA. It is widely studied with extensive literature to rely on but is highly invasive and not representative of physiological injuries due to artifacts from the surgical incision. Although it allows for controlled onset of PTOA, the rapid progression and exposure to the environment can make it difficult to capture early changes in the metabolic profiles. Surgical destabilization of the medial meniscus (DMM) mimics meniscal injuries, which are clinically common and strongly liked to OA. DMM progresses a bit slower than ACL transection, closer to human OA progression, which allows for a better understanding of early changes. However, DMM is still highly invasive, and surgery introduces variability into the sample pool. Medial meniscal transection (MNX) will not be reviewed in this thesis due to decreasing usage in the literature and the monoiodoacetate (MIA) model of OA pain will be discussed later.

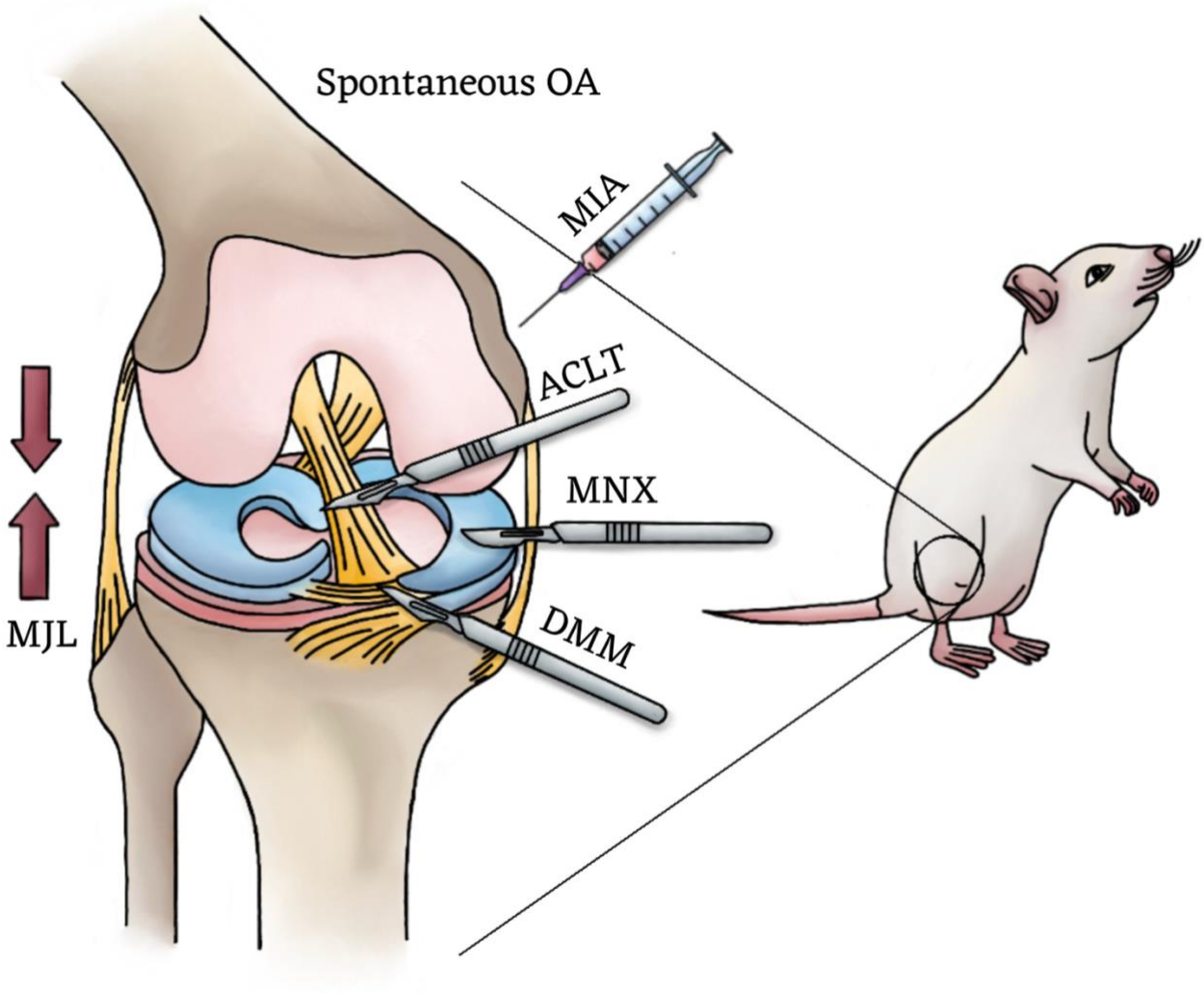

Figure 4: Cartoon image of mice surgery. Mechanical Joint Loading (MJL), MonoIoodoacetate Injection (MIA), Anterior Cruciate Ligament Transection (ACLT), Mitochondrial-Nuclear Exchange (MNX), Destabilization of the Medial Meniscus (DMM) [26]

Mechanical joint loading (MJL) has become an area of interest in OA research. It is becoming clearer that cartilage homeostasis is mechanically driven and metabolically regulated. MJL can be non-invasive, strictly controlled, and highly repeatable. In mouse models MJL closely replicates high-strain, high-strain rate events representative of sports injuries or trauma. It allows for precise control of loading magnitude, rate, and location. It can be applied to animal joints or to cartilage explants. Most *in vitro* mechanical loading studies rely on utilizing joint

explants, either calf or human OA cartilage. These studies look for changes in matrix turnover, proteoglycan loss, and inflammatory responses [27, 28]. While these are actionable measures to study, they are downstream effects of the direct response chondrocytes have to different loading profiles. Metabolite production in response to loading provides a direct physiological readout of the state of the cartilage [29].

The first step in studying metabolic profiles of chondrocytes *in vitro* is to isolate the chondrocyte from its matrix. In this project, bovine knees from a local abattoir or human knee tissue from patients that have undergone total joint arthroplasty will be referred to as the donors. Through a series of enzymatic digestion and washes the chondrocytes are isolated from their matrix (see Chapter 3 methods) [30]. Then chondrocytes are expanded in two-dimensional monolayer until they reach 70-80% confluency. To injure the chondrocytes, we must suspend them in a 3D environment. *In vivo* The PCM directly surrounds the chondrocytes, so the 3D structure should ideally mimic the mechanical and structural properties of the PCM.

Low-gelling-temperature agarose hydrogels provide a controllable, 3D environment that mimics the key mechanical and transport features of cartilage that suites *in vitro* studies of mechanobiology in chondrocytes. Applying mechanical deformations to chondrocytes in a reproducible 3D environment allows for controlled experimentation, and well-defined input displacements. It also allows for less obstructive metabolomics studies, isolating chondrocytes as the only influence on metabolism in the sample. For example cartilage explants display inherent variations in the material and structural properties. Cartilage samples from multiple donors have different stiffnesses; when applying the same mechanical load to explants from different donors, the transduced load to the chondrocyte will be different. By using the same 3D environment, we

limit variation in the force experienced by the chondrocytes under applied deformation and therefore limit overall variability.

Agarose has a tunable stiffness, based on concentration. Increasing the percentage of agarose concentration in the gel yields a higher stiffness. To mimic the PCM of cartilage a 4.5% wt/vol agarose hydrogel is utilized in this research. Agarose is also an inert polymer, meaning it has minimal bioactivity. Therefore, suspending chondrocytes in agarose provides a three-dimensional biochemical scaffold that has minimal effects chondrocyte physiology [31].

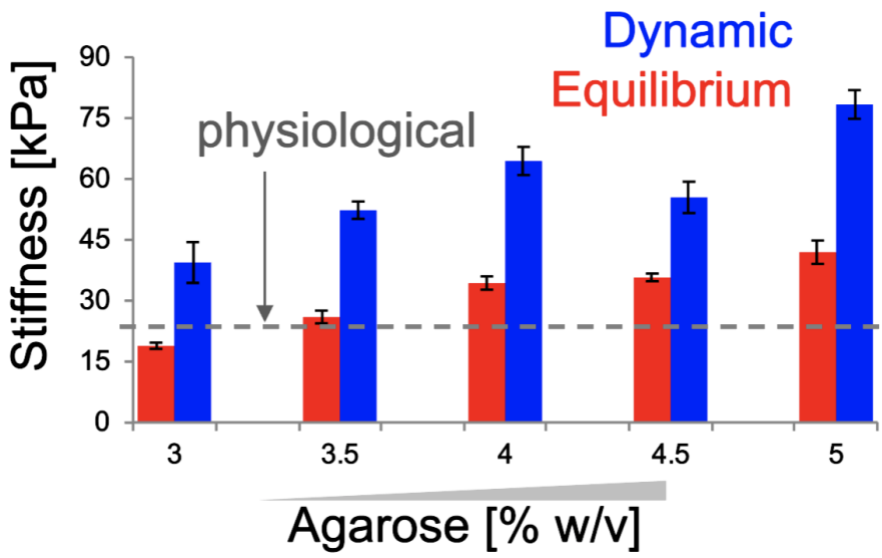

Figure 5: Physiologically stiff agarose [32]

Pathway Inhibition

Targeting central carbon metabolism provides a mechanistic approach to test how chondrocyte metabolism responds to dynamic loads. Chondrocytes rely heavily on different metabolic pathways, including glycolysis and oxidative phosphorylation, to maintain the ECM [19, 33]. Disruption of these pathways occurs in early stages of OA. Targeting specific

metabolites in central carbon metabolism provides a powerful approach to assess the role of metabolism in regulating cellular responses to mechanical stimulation. Small molecule inhibitors can serve as precise probes to study glycolysis and associated pathways. By selectively inhibiting certain pathways these tools allow us to test hypothesis that metabolic activity is an active driver of cartilage phenotype. In this project we study metformin (MET) and monoiodoacetate (MIA). This strategy allows us to create a framework for how metabolic profiles are linked to functional outcomes, providing clarity on potential targeted therapeutics for OA.

Metformin Mechanism of Action

Metformin is a widely used antidiabetic drug, that acts through both activation of AMP-activated protein kinase (AMPK) and inhibition of mitochondrial complex I. This activity alters chondrocyte energy metabolism and inflammatory signaling. Research shows that maintaining AMPK activity in chondrocytes its critical for maintaining ECM homeostasis [34]. Metformin (MET) does not directly regulate AMPK activity but instead acts indirectly by inhibiting mitochondrial complex I, which then regulates AMP levels which control AMPK activity. Metformin is associated with reduced inflammatory signaling and could be used as a pain management drug for OA. In higher concentrations (>20μM) over longer time periods (>24hrs) MET has been shown to lead to cell death [35]. For our purposes however, on the metabolic level, MET can lead to insights on how experimental stimuli such as injury alter chondrocyte metabolism when respiration is inhibited. This information can advance knowledge of the mechanobiology of chondrocytes.

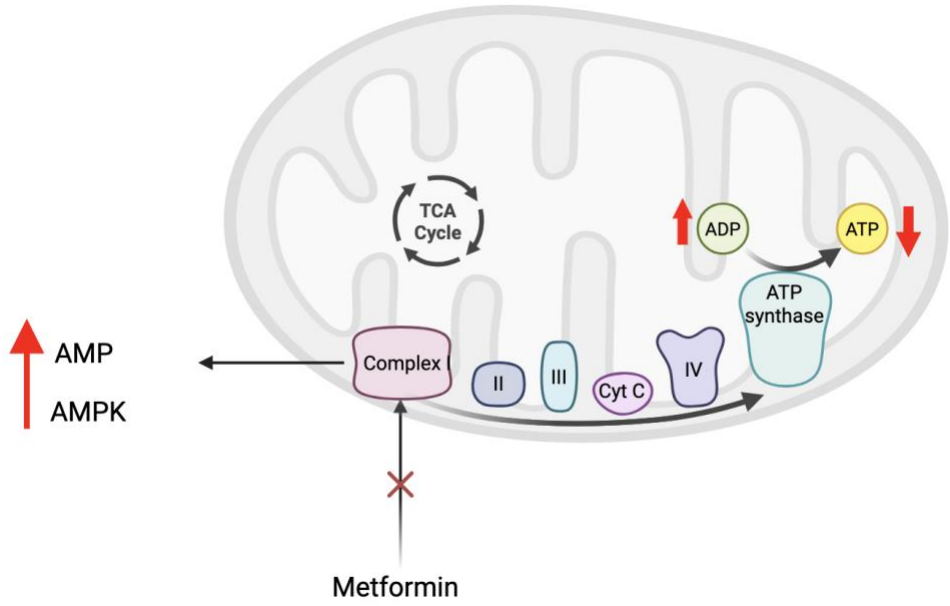

Figure 6: Mechanism of Action Diagram, Metformin

Iodoacetate (MIA) Mechanism of Action

In contrast to MET, MIA irreversibly inhibits glyceraldehyde-3-phosphate dehydrogenase (GAPDH), dramatically reducing glycolysis. GAPDH is a central glycolytic enzyme that catalyzes the conversion of glyceraldehyde-3-phosphate (G3P) to 1,3-bisphosphoglycerate. This reaction couples carbon flux through glycolysis with the reduction of NAD+ to NADH, linking energy production to redox balance. By driving this step GAPDH enables downstream substrate level phosphorylation events that generate ATP and certain cellular metabolites in chondrocytes [36]. MIA treatment leads to cell death, ATP depletion, and increased oxidative stress [37].

Historically MIA has been used to induce OA in rats and mice. This process is done by injecting MIA into the knee joint (Figure 4), causing rapid pain-like responses. The resulting changes in the knee joint, and animal behavior are similar to some of the characteristics of

human OA patients, including pain and pathology [38]. In this project we will not be using MIA to onset disease progression. Rather, we will be using it as another tool to inhibit pathways in metabolism. By comparing how MIA-treated chondrocytes and controls can provide insight into the role of glycolysis in chondrocyte mechanotransduction.

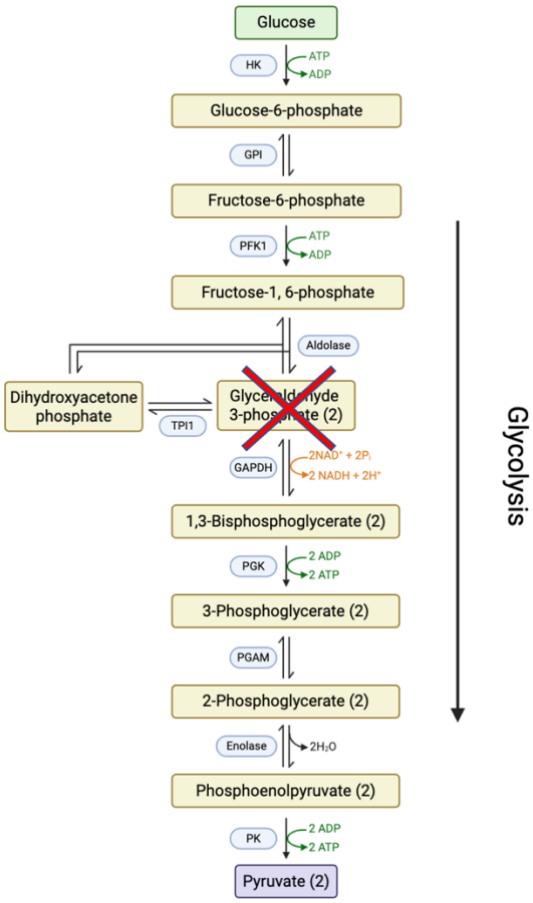

Figure 7: Mechanism of Action Diagram, MIA

Objective and Thesis Outline

In summary, the overall goal of this research is to better inform future studies on the role of central metabolism in chondrocyte mechanotransduction. Specifically, the role of normal and

injurious mechanical stimulation on the metabolic profiles of chondrocytes will be examined. By integrating *in vitro* mechanical testing with targeted metabolomics, this work aims to identify how different mechanical stimuli affect central metabolism in human OA and normal bovine chondrocytes. Defining these changes in chondrocyte mechanotransduction may lead to insight into the mechanobiology of how chondrocytes respond to injury, as well as how or inhibition central metabolism affects the response to mechanical stimulation. These insights could inform future therapeutics or strategies for cartilage repair in OA and/or PTOA.

The remainder of this thesis is organized as follows:

- Chapter 2: Injury Characterization, preliminary work for modeling injury loading conditions in agarose hydrogel system.
- Chapter 3: Injury Causes Altered Metabolism and Oxygen Consumption in Bovine and Human Chondrocytes, presents a manuscript for publication.

CHAPTER TWO

2.0 INJURY CHARACTERIZATION

Historically injury models are invasive *in vivo* methods that subject mice or rats to destabilizing surgery or toxic injection. While mouse and rat models provide a useful tool for studying tissue level and whole joint responses, they are complicated by the plethora of cell types and tissues that interact through complex and unknown mechanisms. For example, external joint loading is a non-invasive method of applying injury *in vivo* and offers a less invasive path to injury and the onset of PTOA than surgical models [39]. While more controlled than surgery, the non-uniformity of specific joints and plethora of cell types introduces variability that is difficult to correct for in statistical processing. In contrast, *in vitro* studies allow for tighter control of inputs and environmental conditions.

The objective of this chapter is to characterize a novel *in vitro* injury model. To control for both input variability and joint variability, we use the previously described agarose hydrogel system. An overview of the workflow for applying *in vitro* injury in an agarose hydrogel model is shown in Figure 8 below. Here we describe the methods development for applying injurious compression to agarose-encapsulated chondrocytes, measuring oxygen saturation in these samples, and extracting metabolites for mass spectrometry.

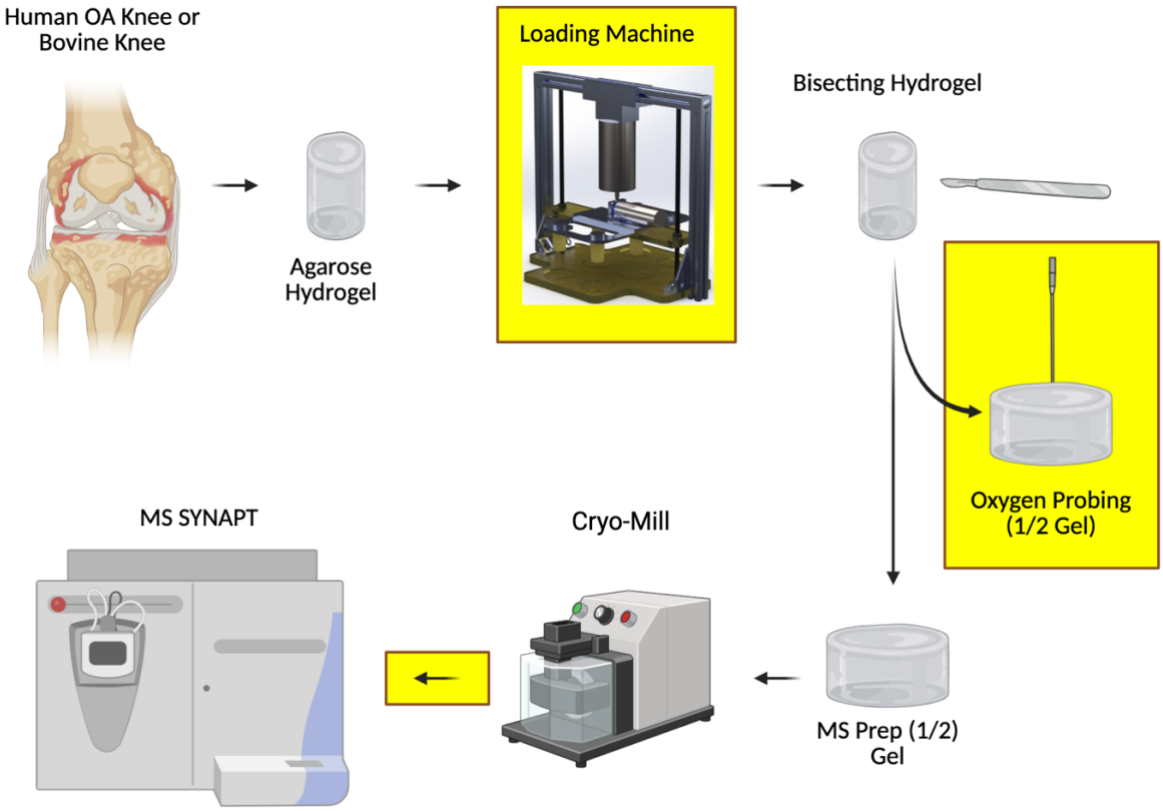

Figure 8: General workflow of agarose hydrogel system, Highlighted portions are the uncharacterized work, that were validated prior to study.

Injurious Loading Conditions

Grodzinsky and Patwari showed tissue levels changes when applying a strain magnitude of 65% at a strain rate of 400%/s to human cartilage explants [27]. This resulted in proteoglycan loss, inflammatory responses, and cell death that are consistent with the onset of PTOA. A strain magnitude of 65% applied in a single cycle was used in this experiment because it produced peak levels of stress that showed macroscopic tissue level damage to the cartilage explants [27].

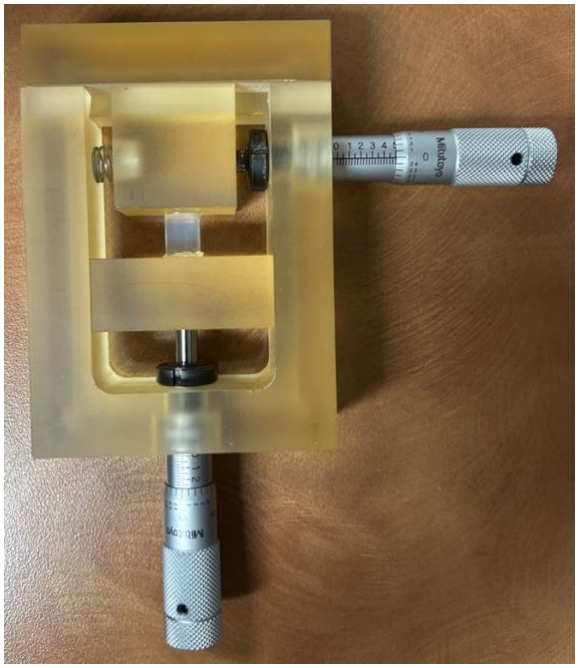

Figure 9: Pilot 1 Apparatus

To implement these loading parameters in an agarose hydrogel system, the strain rate of 400%/s was used. However, the total strain magnitude was limited by fracture of the agarose hydrogel in pilot studies (data not shown). To understand the total strain before hydrogel fracture, a second exploratory pilot study was performed. Using a custom machined block with micrometer-controlled strain actuators, the total strain before fracture was assessed.

A total of 6 hydrogels were assessed macroscopically and qualitatively to identify the failure type and condition (Table 1). This pilot test had many limitations, exposure to air (bench work), uncontrolled strain rate, and sample dehydration due to exposed air during the experimental loading (note that the gels were removed from PBS just prior to loading in this pilot experiment).

Table 1: Qualitative Results on Pilot 1

Sample #	L_0	L_i	E	Break notes	Test Notes	Conclusion
1	507	198	0.39	crack	"Fast"	NA
2	506	100.5	0.19	Slipped/fractured	NA	Didn't dry off plastic
3	507	100	0.19	Slipped/fractured	NA	Didn't dry off plastic
4	507	162	0.31	Crack	NA	Didn't dry off plastic
5	506	115	0.2268	No break once reached, after sitting it cracked	"Fast"	NA
6	507	115	0.2268	No break once reached, after sitting it cracked	"Slow"	NA

To better assess these loading conditions a follow up study was performed. A compressive strain of 65% applied at a strain rate of 4 s^{-1} generated peak stress levels that have been shown in previous studies to induce visible damage to cartilage explants that are consistent with injury. To achieve similar conditions to Grodzinsky and Patwari, a total strain energy of 65% was used.

To test these conditions in final experimental environment, a custom built loading device was used. The goal was to assess strain levels and strain rates that result in gel fracture. Four experimental groups were used, varying the maximum compressive strain from 25% to 35% and the strain rate from 3 s^{-1} to 4 s^{-1} (Table 2).

Table 2: Preliminary Parameters for Injury Condition for Metabolomics Study

37C : 5% CO_2 : 20% O_2					
# Of Cycles	Strain Rate (s^{-1})	Strain Total (%)	Preload (%)	Strain Energy (%)	Fracture?
7	3	25	5	65	No
7	3	25	5	65	No
5	4	30	5	65	No
5	4	35	5	77	yes

This loading was done with strict adherence to experimental conditions and the following parameters were chosen for the final experiment.

Table 3: Final Parameters for injury condition for metabolomics study.

$\dot{E}(t)$	Strain Rate	4 second-1
E_E	Total Strain Energy	65%
Cycles	Cycles	4.8 = 5
$V(t)$	Velocity	51.2mm/s or 2in/s
Temp	Temp	37C
CO2	Carbon Dioxide	5%
O2	Oxygen	20%
Preload	Strain Magnitude	5%
Final (+preload)	Strain Magnitude	30%
		Success.

Oxygen Consumption

Now that we have specified the parameters of the injury model (*i.e.* total strain, strain rate, and number of loading cycles), we must verify the process to measure oxygen consumption. Oxygen microelectrodes and affiliated software (UNISENSE, Aarhus, Denmark) was used to

quantify oxygen saturation. These probes function by changing electrical resistance when exposed to different levels of oxygen saturation. Under constant current, the resistance of the probe changes when exposed to different O_2 levels, and the output voltage is measured. For calibration, the probe is submerged in water with 0% oxygen and the output voltage is recorded. Then the probe is submerged in water saturated with oxygen, and a two-point calibration curve is established.

From this calibration curve the output voltage of the probe when inserted into the samples (*e.g.* agarose hydrogel) can be mapped to a specific concentration of oxygen. However, difficulties arise when considering the temporal response of the probe. The temporal response of the probe has potential to induce measurement error. To address this, measurements were recorded at 10 Hz over 5 minutes within agarose samples. Oxygen saturation decreases as the probe breaks the gel-atmosphere threshold, then continues to a low point and increases when the gel, exposed to the air, is overcome by the diffusion of the oxygen in the air to the gel. Statistical modeling showed that there was no difference ($p<0.05$) between the average reading of 5, 10 or 15 seconds or utilizing the low point as the final value. (Table 4).

Table 4: Pilot study showing no difference in average readings of O2 saturation over time.

Comparison	P – Value	Significance
5-seconds Vs 10-seconds (no PBS)	1	No difference
5-seconds Vs 10-seconds (PBS)	1	No difference
5-seconds Vs 15-seconds (no PBS)	0.99374	No difference
5-seconds Vs 15-seconds (PBS)	0.99584	No difference
10-seconds Vs 15-seconds (no PBS)	0.9944	No difference
10-seconds Vs 15-seconds (PBS)	0.99629	No difference
Low-point Vs 5-seconds (no PBS)	1	No difference
Low-point Vs 5-seconds (PBS)	1	No difference

Thus, we chose minimum value for our measurements. This standardization lowers the chance for random error due to variations in the temporal signal from the oxygen probes.

The second problem arises when considering process time within an experiment. Because our testing protocol simultaneously applies mechanical stimuli to 6 gels at once, challenges arise at the end of an experiment when all 6 samples come off the machine at the same time. Leaving gels on the bench or in the incubator would introduce additional error. Based on the experimental design of the following study this problem does not persist. Only one gel in the following study is processed at a time, so processing multiple gels at once is not taken into consideration here. However, process time is not fully mitigated. Recall that the gels must be used for both mass spectrometry and oxygen saturation. Inserting the oxygen probe into the gels will introduce additional forces that are not part of the specified mechanical stimulus. While

probing, the embedded chondrocytes will continue to metabolize well past their designated experimental timepoint. To mitigate this, gels are bisected, and one half is immediately flash frozen in liquid nitrogen while the other is utilized for oxygen measurements. This will be explained more in Chapter 3.

Metabolite Extraction

After the gel is flash frozen it is subsequently pulverized using a hammer, plunger, and metal fixture. This pulverization increases the ratio of surface area to volume, allowing more efficient metabolite extraction into the solvent. After the gel is pulverized, it is transferred to a Cryo-Mill (RETSCH, Haan, Germany). The Cryo-Mill, cooled by liquid nitrogen, brings temperatures down to -196°C and shakes laterally. The sample is sandwiched between two ball bearings and the lateral movement of these ball bearings pulverizes the gel into a fine powder. The goal of this is to increase the gels surface area to volume ratio (e.g. small pieces) while keeping the temperatures as low as possible to avoid metabolite evaporation. Directly after cyro-milling the powder is suspended in a buffer that extracts the metabolites from the agarose. Agarose is a natural polysaccharide extracted from seaweed and carries a slight negative charge at physiological pH. There are some metabolites of interest that are positively charged, leading to separation problems.

Typical metabolite extraction methods utilize ~5mL of 70:30 methanol:acetone to be added to the powder. However, to address our objective we need to target as many metabolites as possible, which is 17 metabolites from central metabolism. These 17 are precursor, and branching-point intermediates that serve as essential building blocks for protein synthesis. Thus, there is no room to miss any metabolites during the extraction step. The first step to solve this

problem is to protonate the agarose to screen the negative charge that might bind metabolites. The first test was 70:30 methanol:acetone with 1% hydrochloric acid. This extraction method proved to be too strong of an acid leading to a brown/black buffer and thickening the solution which is not compatible with mass spectrometry. Switching to a 70:30 methanol:acetone with 1% formic acid showed a lighter more diluted solution observationally similar to the original buffer without the acid.

Further analysis using targeted mass spectrometry detected 16 of 17 metabolites of interest while using the 1% formic acid method. This is a distinct increase from 12 of 18 metabolites of interest detected without formic acid. The addition of salt was also a consideration. However, desalting methods proved inadequate to remove sufficient salt for mass spectrometry.

CHAPTER THREE

INJURY CAUSES ALTERED METABOLISM AND OXYGEN CONSUMPTION

Contribution of Authors and Co-Authors

Manuscript(s) in Chapter(s) [#]
Author: Aidan Gregory
Contributions: Experimental Design, Data Collection, Data Analysis, manuscript drafting and revisions.
Co-Author: Priyanka Brahmachary, PHD
Contributions: Data Collection, Data Analysis, manuscript drafting and revisions.
Co-Author: Liam Rockwell
Contributions: Data Collection, Data Analysis
Co-Author: Molly Piazza
Contributions: Data Analysis
Co-Author: Emelia Keim
Contributions: Data Collection
Co-Author: Belle Anselmo
Contributions: Data Collection
Co-Author: Erik Myers, PHD
Contributions: Experimental Design
Co-Author: Ross Carlson, PHD
Contributions: Experimental Design, Data Interpretation
Co-Author: Ronald June, PHD
Contributions: Experimental Design, Data interpretation, Manuscript Drafting

Manuscript Information

Aidan Gregory, Priyanka Brahmachary, Liam Rockwell, Molly Piazza, Emelia Keim, Belle Anselmo, Erik Myers, Ross Carlson, Ronald June
Status of Manuscript:
☒ Prepared for submission to a peer-reviewed journal
☐ Officially submitted to a peer-reviewed journal
☐ Accepted by a peer-reviewed journal
☐ Published in a peer-reviewed journal

Abstract

Traumatic joint injuries both disrupt chondrocyte metabolism and increase the risk for post-traumatic osteoarthritis. Yet the relationships between trauma, altered metabolism, and cartilage degradation remains unclear. This study compares the metabolic responses of bovine and osteoarthritic (OA) chondrocytes to physiological and injurious mechanical stimuli under normoxic (20% O2) and hypoxic (5% O2) conditions. Using primary chondrocytes encapsulated in agarose, physiological and injurious mechanical stimulation, targeted metabolomic profiling of central carbon metabolites, and oxygen saturation measurements, these data find that healthy bovine chondrocytes exhibit robust, time-dependent adaptation to mechanical stimuli, whereas OA chondrocytes display a blunted response, particularly under injury conditions. Injurious mechanical stimuli led to altered oxygen consumption and glutamine accumulation, suggesting disrupted glycolytic flux and mitochondrial dysfunction in OA cells. These findings underscore the role of mechanical cues in chondrocyte metabolism and inform future studies aimed at identifying metabolic targets relevant to PTOA progression.

Introduction

Osteoarthritis (OA) is the leading global cause of disability, affecting over 600 million people worldwide, characterized by the progressive degradation of articular cartilage [1, 2]. Traumatic joint injuries increase risk for the development of osteoarthritis: isolated anterior cruciate ligament (ACL) injuries account for an estimated 12% of all OA cases, while multi-tissue injuries account for 48% of cases [40]. This form of OA, known as post-traumatic osteoarthritis (PTOA), develops from joint trauma, often due to altered joint mechanics and

abnormal cellular responses [25]. Despite the high prevalence of PTOA, cellular mechanisms linking injury to cartilage degradation are not fully understood.

Articular cartilage provides a smooth, low friction surface that facilitates joint movement while distributing mechanical loads in the joint [41]. Chondrocytes, the sole cell in articular cartilage, are responsible for synthesizing and maintaining the extracellular and pericellular matrices (ECM and PCM, respectively). Unlike most tissues, articular cartilage is avascular and exists in a hypoxic environment with oxygen tension below ~5% [5]. Importantly, synthesis of key amino acid precursors for both the ECM and PCM stem from central carbon metabolism. In vivo, the ECM and PCM transmit mechanical forces to the chondrocytes. This mechanotransduction influences chondrocyte metabolism and matrix homeostasis. However, excessive mechanical forces, such as those that develop during traumatic joint injury, can shift chondrocyte metabolism toward matrix catabolism, reducing their ability to regulate and maintain cartilage integrity [42, 43].

Central carbon metabolism – which includes glycolysis, the pentose phosphate pathway (PPP), and the tricarboxylic acid (TCA) cycle – synthesizes the precursors to non-essential amino acids. This plays a critical role in maintaining the articular cartilage by supplying the precursors needed for synthesis of ECM and PCM molecules. Glycolysis converts glucose into pyruvate and ATP thus supplying energy for cellular processes. Pyruvate is converted to acetyl-CoA and enters the TCA cycle which produces most of the amino acid precursors necessary for PCM and ECM synthesis. Dysregulation of these pathways can lead to an imbalance between anabolic and catabolic activity of the ECM and PCM. In OA cartilage, chondrocytes exhibit increased matrix catabolic activity that disrupts the balance between matrix synthesis and

degradation [44, 45]. Healthy chondrocytes, however, generally maintain matrix homeostasis, which is supported by physiological mechanical stimulation [46]. The extent to which mechanical injury alters specific pathways of central metabolism, and how this is altered in OA, remains unclear.

While previous studies characterized macroscopic and microscopic tissue changes following joint injury [27, 28], the intracellular metabolic response, particularly that involving central carbon metabolism, remains poorly defined, and the direct metabolic response of chondrocytes to mechanical injury has yet to be fully characterized. This gap limits our ability to develop targeted interventions to increase metabolic production of non-essential amino acid precursors toward preserving cartilage health post-injury. Therefore, the objective of this study is to define the metabolic responses of chondrocytes to mechanical injury. We hypothesized that injurious stimulation will induce a metabolic shift favoring anaerobic metabolism, characterized by an increase in lactate production and altered oxygen consumption, whereas physiological stimulation will produce metabolites that maintain matrix homeostasis.

This study uses primary bovine and human OA chondrocytes embedded in high-stiffness agarose. Independent variables include physiological or injurious compression and normoxic or hypoxic tissue culture. Dependent variables include oxygen consumption and concentrations of central metabolites measured using targeted metabolomics. By identifying metabolic changes associated with in vitro mechanical injury, this study seeks to provide insight into chondrocyte mechanotransduction to inform potential future therapeutic strategies for PTOA prevention.

Methods

Chondrocyte Harvest and Sample Preparation

Human Primary Chondrocytes (HPC) were obtained from discarded arthroplasty tissue from Stage-IV osteoarthritis patients undergoing total joint replacement under IRB approval. Bovine chondrocytes were harvested from knee joints of 18-22 month old cattle obtained, from a local abattoir. Briefly, tissue was digested with Type I Collagenase (2 mg/mL) (Gibco, Waltham, MA, USA) for 14 h at 37 ºC using a previously established protocol (1). Isolated chondrocytes were cultured in Dulbecco's Modified Eagle's medium (DMEM) (Gibco, Waltham, MA, USA) supplemented with Fetal Bovine Serum (FBS) (10% v/v) (Bio-Techne, Minneapolis, MN, USA), penicillin (10,000 I.U./mL), and streptomycin (10,000 µg/mL) (Sigma, St. Louis, MO, USA) in 5% CO2 at 37 ºC and first passage population was used for experiments.

Cells were washed with 1X PBS and resuspended in DMEM (devoid of Phenol Red) and mixed with low melting temperature agarose Type VII-A (Sigma Aldrich) at a final concentration of 4.5% wt/vol with ~500,000 cells/gel and allowed to solidify for 10 min. Agarose gels were placed in a 24-well tissue culture plate (Falcon) with 2 mL custom DMEM media containing 4.5g/L glucose, 2 mM L-glutamine, 110mg/L sodium pyruvate, 10% FBS, and 1% PenStrep and cultured overnight in 5% CO2 at 37ºC.5

To mimic the PCM in an in vitro 3-D model, articular chondrocytes were suspended in 4.5% wt/vol type VIIA low-gelling temperature agarose using previously described methods [27, 47]. A total of 90 gels from n=10 ten bovine samples, and 90 gels from n=10 ten human OA donors were created. Because phenol red interferes with mass spectrometry (see below), gels were equilibrated in phenol-red-free (white) DMEM supplemented with 10% FPS, 1% PenStrep,

4.5g/L glucose, 2mM glutamine, and 110mg/L sodium pyruvate for 24 hours under standard tissue culture conditions (normoxic 20% O_2 or hypoxic 5% O_2 with 5% CO2 at 37°C) [15]. 1 hour prior to mechanical stimulation samples were submerged in 5mL of Phosphate Buffered Saline (PBS).

In Vitro Mechanical Stimulation and Injury

Gels from each donor were divided into 3 mechanical stimulation groups: injury, physiological, and control.

To identify the necessary loading conditions — the magnitude of compressive strain, strain rate, and number of loading cycles — a strain energy calculation was performed. Grodzinsky et al previously established an in vitro injury model for explants of articular cartilage. In this model a compressive strain of 65% is applied at a strain rate of 4 s-1. This induces macroscopic damage to cartilage explants that is consistent with injury [12]. In pilot studies, we observed that agarose samples fracture at strains above 30%. Using a custom-built loading device (Figure 1A), a preload of 5% static compressive strain was applied for 15 minutes [16]. To simulate the Grodzinsky injury model, a total strain of 65% was then applied by subjecting hydrogels to an additional 25% strain for 5 cycles at a frequency of 6.6Hz (strain rate of 4 s^{-1}). For the physiological control, the same total strain of 65% was achieved using 42 cycles at 5% strain amplitude at a frequency of 1.1 Hz (strain rate of 0.346s^{-1}). We used an additional control group of unloaded gels.

Measurement of Oxygen Consumption

Mitochondria utilize redox carriers generated in the TCA cycle to generate ATP. Because mitochondrial respiration requires oxygen, oxygen saturation testing was performed to

characterize differences in mitochondrial activity and overall metabolic activity between groups. Alterations in oxygen consumption indicate shifts in mitochondrial respiration that can represent metabolic changes in activity of the TCA cycle, pentose phosphate pathway (PPP) or anaerobic glycolysis [43]. Pilot data found that processing multiple gels simultaneously influenced the oxygen saturation of the gels. Therefore, one gel per donor was processed for each timepoint to ensure accurate readings across experimental groups. After loading, hydrogels were bisected. One half of each gel was processed for metabolomic profiling by flash freezing in liquid nitrogen while the remaining half was immediately probed for oxygen saturation. To characterize time-dependent metabolic shifts after mechanical stimulation, hydrogels from all experimental groups were reintroduced to culture conditions in white DMEM (as described above) for 0, 1, 4, or 24 hours prior to oxygen testing and metabolomic processing.

Oxygen testing was performed using UNISENSE (50 micron) oxygen probes (UNISENSE, Aarhus, Denmark) and logger software (Figure 1B). Probe locations were estimated to be at the center of the sample with a tolerance of ±1 mm for both radial and axial directions. The minimum value of oxygen saturation was used after a pilot study found no statistical differences ($p < 0.05$) from an average of 5, 10, or 15 seconds of sampling.

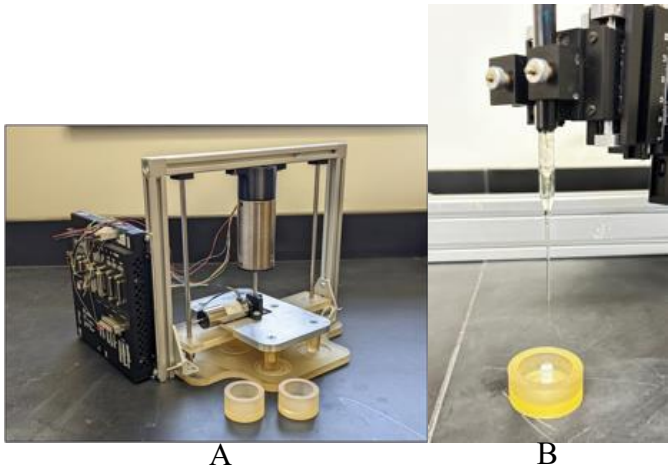

A B

Figure 1: A. Custom built loading machine B. Probing a hydrogel with UNISENSE oxygen probe

Metabolite extraction

After mechanical stimulation (or unloaded control), samples were flash frozen and pulverized before storage at –80°C for 12 hours. Samples were then homogenized using a temperature controlled CryoMill (RETSCH, Haan, Germany) for a total of 12 minutes, and subsequently dissolved in 5mL of 70:30 methanol:acetone with 1% formic acid for 12 hours. All reagents for metabolite extraction were HPLC-grade or higher. The buffer was centrifuged at 4000 rpm for 10 minutes then removed from the hydrogel by pipetting. To isolate the metabolites from the supernatant a vacuum concentrator at 45°C was used, until only sediment remained. Samples were then stored at –80°C until mass spectrometry [47].

Metabolomic Profiling

To investigate how mechanical stimulation can impact Central Carbon Metabolism (CCM), a targeted panel of 17 key central metabolites was developed (Supplementary Table 1).

These included glucose, pyruvate,8 lactate, oxaloacetate, and glutamine. Glucose, the primary substrate for glycolysis, and pyruvate, a critical glycolytic product, were quantified to assess glycolytic activity. Pyruvate serves as a metabolic branching point, converting either to lactic acid or acetyl-CoA, which feeds the start of the TCA cycle. The TCA cycle can metabolize acetyl-CoA into oxaloacetate, a precursor for lysine, which contributes to synthesis of collagen, a key constitutent of both the PCM and ECM. Additionally, glutamine and proline are precursors for collagen. Collagens (type II and VI) are critical for the structural integrity of the ECM and PCM, highlighting the importance of these metabolites in supporting cartilage function under mechanical stimuli.

To quantify metabolomic changes, a targeted metabolomics approach was employed. Calibration standards were prepared using each of the 17 metabolites of interest at concentrations of 1, 2, 10, 50, and 100 µg/µL suspended in 50mL of 50:50 acetonitrile:HPLC water. Experimental samples were suspended in 10 µL of the same solvent and vortexed for one minute [47].

Metabolite analysis was performed using high-performance liquid chromatography-mass spectrometry (HPLC-MS) operating in positive ionization mode (Waters, Synanpt, c18 column). The instrument operated at a resolution of 20ppm, maintaining a mass accuracy of 5ppm. Metabolites were identified and separated based on the corresponding m/z value and retention time through Agilent Mass Hunter Quantitative software. Quantification was achieved by comparing sample metabolite intensities to the prepared calibration standards.

Statistical Analysis of Metabolic Data:

To reduce potential biases and ensure robust experimental design, samples from each donor were randomly assigned to each loading group (control, injury, and physiological) and across all timepoints (0, 1, 4, and 24 hours). Statistical analyses were performed using GraphPad Prism (v10). Oxygen data was analyzed with one-way ANOVAs for intragroup comparisons using Tukey's correction for multiple comparisons.

All metabolite concentration data was normalized to the total ion intensity (TII). Metabolites were then classified into three categories based on detection frequency (<1/3, between 1/3 – 80%, and >80%).

<1/3

If a metabolite was detected in less than 1/3 of samples the metabolite was excluded from all statistical analysis.

1/3-80%

For metabolites detected in one-third to 80% of all sample's donor was removed as a factor because the high number of non-detected caused separation in the model. These metabolites were analyzed using a binomial generalized linear model with loading conditions, injurious and physiological (normal) and time as a factor.

A second binomial generalized linear model was run separately for the 0-hour timepoint, (directly after loading) that included only the loading conditions, injurious physiological and control, as a factor. Type-II ANOVAs were run for both statistical models.

>80%

If the metabolite was detected over 80%, linear models were created, including loading condition (excluding control), time, and donor as factors. Type-II ANOVAs were used to analyze the linear model.

A stepdown modal simplification approach was applied: if the factor with the greatest nonsignificant p-value was donor, it was removed from the model was reanalyzed.

A separate linear model was created at time point 0, directedly after loading, including loading condition (including control) and donor as factors. The same stepdown approach was used to simplify the model, if the effect with the greatest nonsignificant p-value was donor, it was removed from the model and the analysis was repeated. Tukey's multiple correction was used for all type two ANOVAs where a difference was detected.

Results

Oxygen Saturation

We measured oxygen saturation levels using microelectrodes because oxygen is required for mitochondrial respiration to process TCA cycle products.

Normoxic Culture

Hydrogels from unloaded control bovine samples (n=10) displayed significantly lower oxygen saturation than OA human donors (n=6, Figure 2A). Post-injury, hydrogels from bovine samples showed higher oxygen saturation compared to human OA donors after 4 hours (Figure 2B).

Hydrogels from bovine samples (n=10) showed a clear oxygen saturation response to both physiological and injurious mechanical stimuli. Increasing in both loading conditions at 1

hour post loading compared to control then decreasing at later timepoints when compared to 1 hour. These changes were persistent across timepoints (Figure 2C). In contrast, hydrogels from human OA chondrocytes did not show changes in oxygen saturation in response to physiological or injury mechanical stimuli over time (Figure 2D).

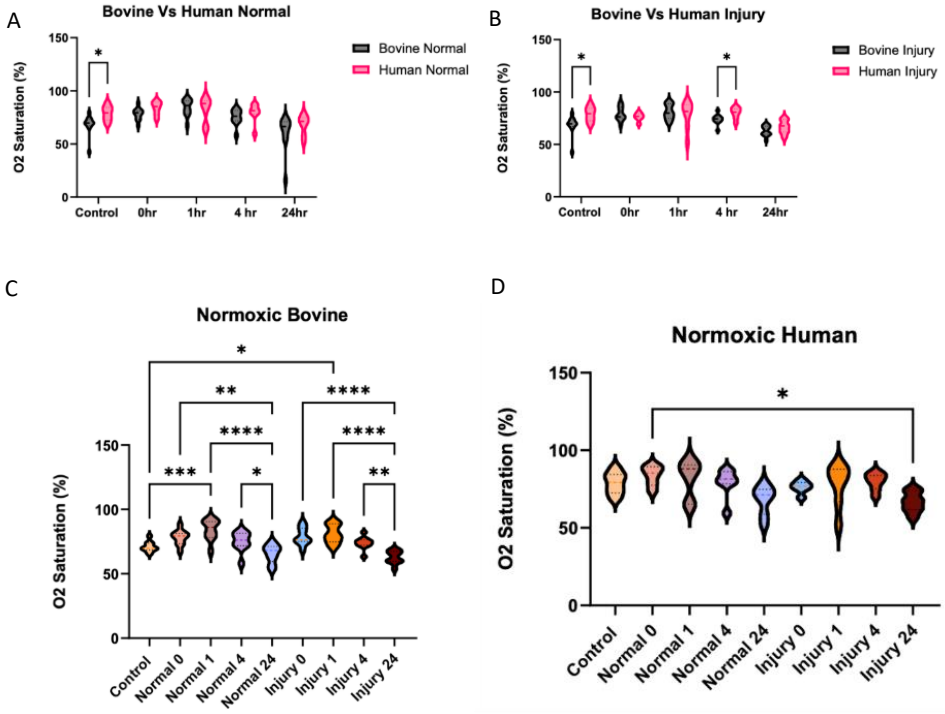

Figure 2: Oxygen saturation (%) levels of chondrocytes under normoxic conditions over time. Panels A and B show oxygen saturations of agarose hydrogels under physiological (normal) and injurious (injury) loading conditions respectively, in normoxic (20% O2) conditions. Panels C and D show oxygen saturations of agarose hydrogels under physiological (normal) and injurious (injury) loading conditions respectively, in normoxic (20% O2) conditions. Violin plots for panel A and B compare the means of each group using two-way ANOVA. Violin plots for panel C and D compares the means of each group using one-way ANOVA. Statistical significance is denoted by the following: $P < 0.05$ = *, $P < 0.01$ = **, $P < 0.001$= ***.

Hypoxic Culture

For samples subjected to physiological mechanical stimulation, human donors (n=3) showed significantly higher oxygen saturation after 4 hours compared to bovine samples (n = 3,

Figure 3A). There were no differences in oxygen saturation for hydrogels from human OA donors at any time point (Figure 3B).

Bovine samples subjected to injurious compression showed a significant decrease in oxygen saturation after 4 hours and 24 hours compared to the unloaded controls. Hydrogels from bovine samples subjected to physiological mechanical compression showed a significant decrease in oxygen saturation at 24 hours when compared to the control. Bovine oxygen saturation at 24-hours was also significantly less than that at 0-, 1-, and 4-hour timepoints (Figure 3C). Hydrogels from human donors subjected to injurious stimulation did not show any significance when compared across timepoints. However, when subjected to physiological stimulation showed a decrease at 24 hours when compared to 0- and 1-hour timepoints. There was a significant decrease in oxygen saturation in human donors at 4 hours compared to 1 hour (Figure 3D).

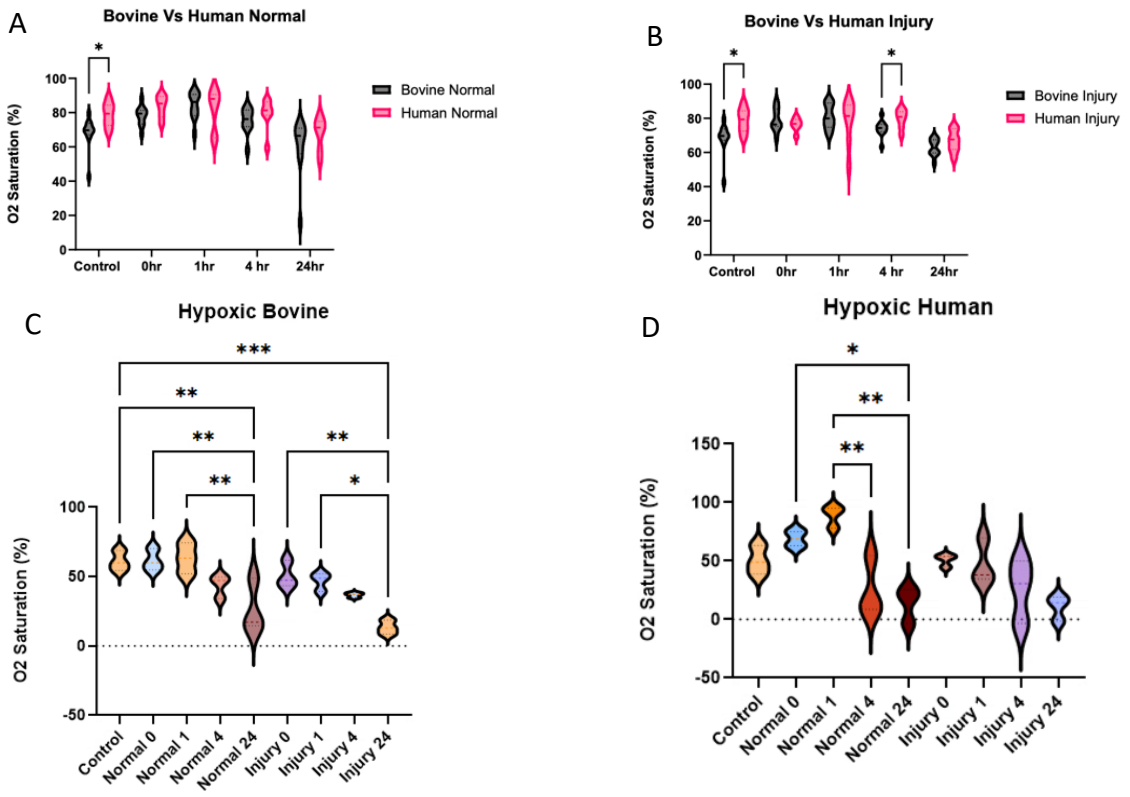

Figure 3: Oxygen saturation (%) levels of chondrocytes under hypoxic conditions over time normalized to 5%. Panels A and B show oxygen saturations of agarose hydrogels under physiological (normal) and injurious (injury) loading conditions respectively, in hypoxic (5% O2) conditions. Panels C and D show oxygen saturations of agarose hydrogels under physiological (normal) and injurious (injury) loading conditions respectively, in hypoxic (5% O2) conditions. Violin plots for panel A and B compare the means of each group using two-way ANOVA. Violin plots for panel C and D compares the means of each group using one-way ANOVA. Statistical significance is denoted by the following: $P < 0.05$ = *, $P < 0.01$ = **, $P < 0.001$= ***.

Metabolite Concentration

Hydrogels from bovine donors (n=10) showed a greater then 50% detection rate in 6 metabolites of interest (Figure 4). Hydrogels from OA donors (n = 10) showed a greater the 50% detection rate in only 3 metabolites (Figure 5).

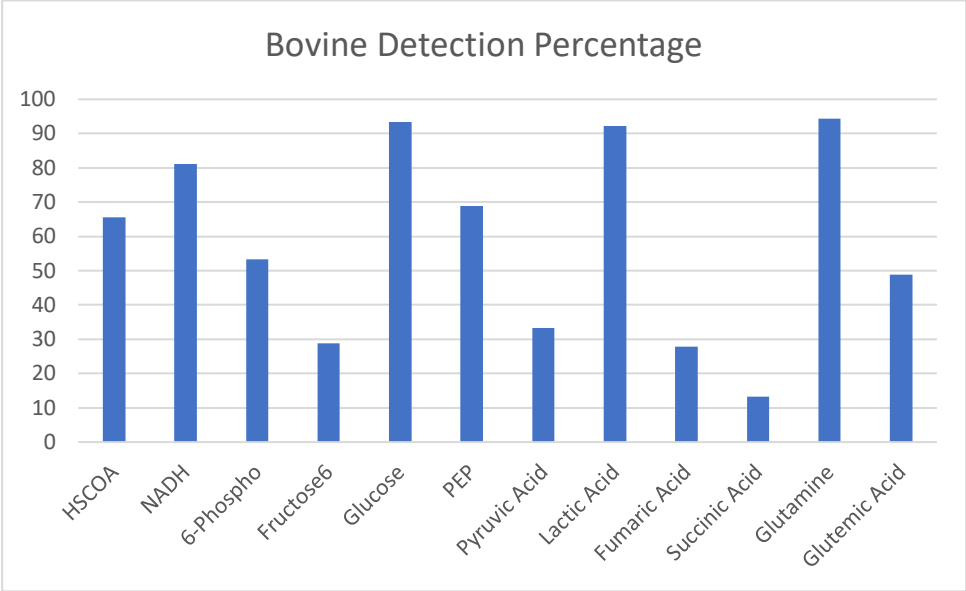

Figure 4: Percentage of Bovine samples that had detected a metabolite (See appendix for full list).

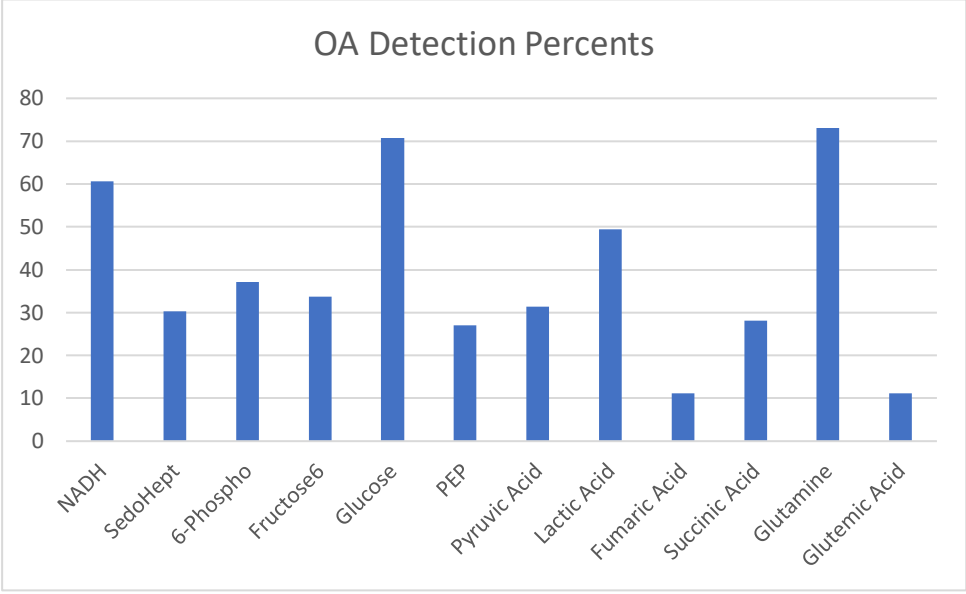

Figure 5: Percentage of OA samples that had detected a metabolite (See appendix for full list).

Bovine donors (n = 10) subjected to injury loading conditions showed an increase in glutamine concentration 4 hours post loading when compared to directly after loading. Bovine

samples subjected to physiological loading also showed increased levels of glutamine concentration 4 hours post loading when compared to directly after loading (Figure 6).

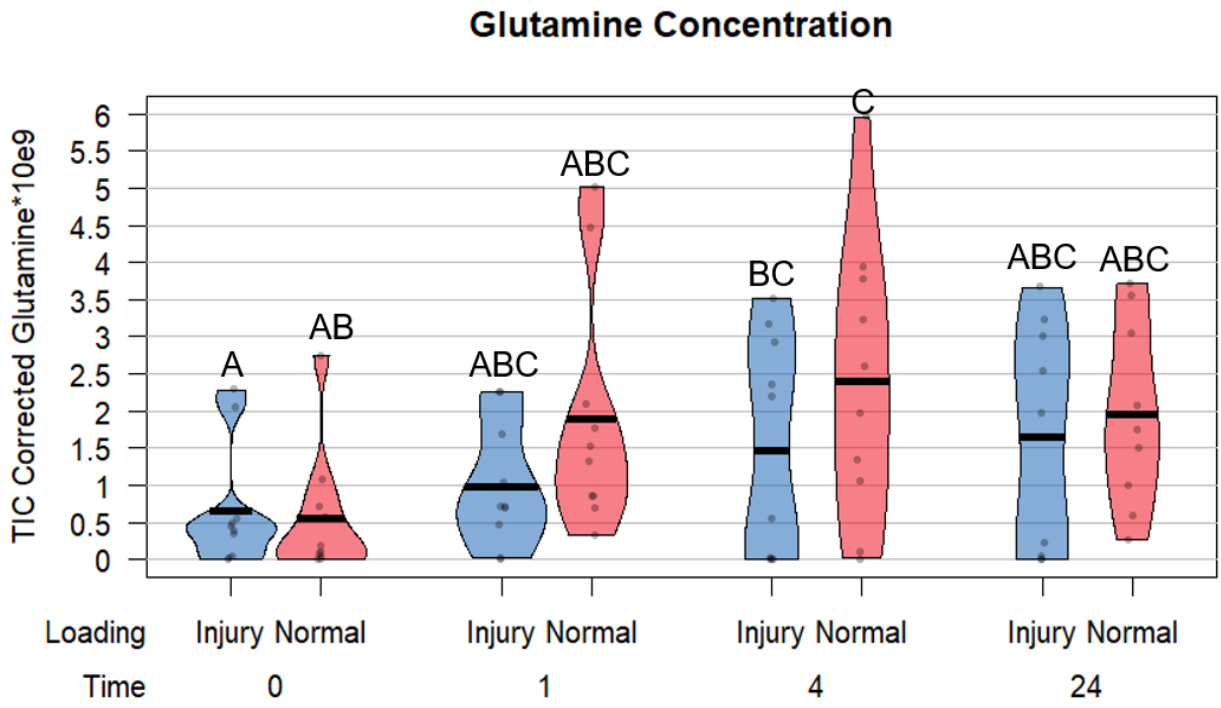

Figure 6: Bovine Donors, Glutamine Concentration TIC corrected. Groups that share one or more of the same letters do not have statistical differences between them.

Discussion

This study aims to evaluate how chondrocytes from different sources (OA and bovine) respond metabolically to mechanical stimulation, under both physiological and injurious conditions. This work integrates mechanical strain parameters with metabolic readouts, including oxygen consumption and metabolite profiles. By comparing healthy chondrocytes with OA chondrocytes in both normoxia and hypoxia this study provides insights into how chondrocytes respond to loading in both healthy and diseased states. Both strain magnitude and strain rate were designed to model physiologically relevant and injurious conditions in vitro. By

characterizing the metabolic state of chondrocytes through quantitative metabolite analysis and oxygen consumption data, this paper shows a metabolic plasticity in response to different loading conditions. These data may have important implications for targeted therapeutics and may inform our understanding of OA progression.

Injury Alters Oxygen Consumption of OA and Bovine Chondrocytes

This study shows clear metabolic distinctions between OA and healthy chondrocytes subjected to injurious and physiological mechanical stimulation. Targeted metabolomics and oxygen consumption data revealed that OA chondrodites exhibit a suppressed metabolic response to injury, in contrast to bovine chondrocytes, that show a robust and time-dependent metabolic alteration under both injury and physiological loading. Notably, in normoxic conditions, bovine chondrocytes responded metabolically as early as one hour post loading, with sustained activity across timepoints (Figure 2C), consistent with an intact capacity for mechanotransduction and bioenergetic adaptation [48].

In contrast, OA chondrocytes displayed minimal changes in oxygen consumption under similar normoxic injury conditions (Figure 3C), indicating a potential mechanotransduction impairment or pre-existing mitochondrial dysfunction [49]. Under hypoxic conditions – more reflective of the in vivo chondrocyte environment - bovine cells exhibited a delayed metabolic response to physiological loading (Figure 2C). Whereas OA cells showed decreased oxygen consumption as early as 1 hour post loading (Figure 3A). This reduction suggests a shift towards anaerobic glycolysis and lactate production, a hallmark of OA cell metabolism, and the fundamental metabolic differences between healthy and degenerative cell phenotypes [50]. It could also indicate no metabolic response at all.

Furthermore, the suppressed response of OA chondrocytes to mechanical injury may reflect a blunted mitochondrial reserve capacity and or reprogrammed metabolic phenotypes incapable of responding to mechanical ques, as supported by previous findings in OA cartilage [51]. Together these data highlight the importance of oxygen metabolism as a functional readout of mechanotransduction and suggest that therapeutic targeting of mitochondrial metabolism could restore chondrocyte responsiveness in OA.

Loading Alters Glutamine Concentration Over Time

The observation of increased glutamine concentration 4 hours post loading when compared to control in normoxic bovine samples suggest a metabolic shift towards enhanced amino acid flux in response to mechanical stress. Glutamine serves as an important metabolic substrate and is an amino acid that can be used in proteins [21]. In the loaded condition, the higher glutamine levels may reflect either accelerated synthesis or reduced utilization of glutamine. When compared directly after loading, a change in concentration shows a metabolic response to both physiological and injurious loading. The mechanical loading may trigger an increase in precursors to structural proteins of the ECM. It has been shown in the literature that glutamine levels increase under stress in highly proliferating cells [52]. Chondrocytes are not highly proliferating but could also show an increase in glutamine as a stress response or to promote collagen synthesis.

Limitations

This study has several limitations that should be acknowledged when interpreting metabolic alterations observed following mechanical injury. First, although bovine chondrocytes provide a consistent and accessible model system, they may not fully represent the behavior of

human chondrocytes, particularly in the context of OA degeneration. Species specific differences in cartilage composition, cell density, and metabolic rate may influence responses to mechanical stimuli and injury.

Second, the in vitro injury model, while enabling controlled application of mechanical loads, does not fully represent the complex physiological environment of the joint, which includes synovial fluid and immune response. The isolated system may exaggerate or underrepresent the expression of certain aspects of the in vitro response to mechanical stimulation.

Third, the use of targeted metabolomics, while advantageous for sensitivity and specificity, limits the scope of metabolic profiling to predefined compounds. The approach may overlook broader shifts in metabolic pathways. For example, while an increase in glutamine was detected post injury, downstream or upstream changes in pathways like the TCA and glycolysis were not detected.

Finally, the interpretations of metabolite levels assume pseudo steady-state flux, which may not be accurate in the context of acute cellular stress or injury.

CHAPTER FIVE

CONCLUSION

This work aimed to characterize the metabolic responses of human and bovine chondrocytes to physiologically relevant and injurious mechanical loading to better understand early mechanobiological events leading to post-traumatic osteoarthritis (PTOA). PTOA is becoming highly recognized as a mechanically driven and metabolically regulated disease. Understanding how chondrocytes respond to different loading conditions is critical for identifying early-stage events that initiate the disease.

By integrating controlled in-vitro loading experiments with targeted metabolomics, this work sought to characterize how different strain magnitudes and strain rates influence chondrocyte metabolism across timepoints. In doing so, this research aimed to fill an important knowledge gap regarding quantified central carbon metabolism responses in a time dependent manor to different forms of mechanical stimulation.

Comparative analysis among bovine and human (OA) chondrocytes revealed key differences in both baseline metabolism and mechanical loading. OA cells showed a less adaptive metabolism, as shown in the oxygen data. Bovine cells showed an adaptive metabolism in both oxygen concentration and glutamine consumption. These findings provide new insight into how mechanical stimuli influence chondrocyte metabolism and highlight the importance of metabolic regulation in cartilage. Overall, this work advances our understanding of cartilage mechanobiology and emphasizes the potential of metabolomics as a tool in orthopedic research.

Building upon these findings, future work should aim to incorporate small molecule inhibitors into the 3-D agarose hydrogel system. This will allow us to study how chondrocytes metabolically respond when access to its full metabolism is limited. Studying this could provide insight into a potential way to guide chondrocyte metabolism away from a disease state to a healthy one.

CUMULATIVE REFERENCES CITED

1. Collaborators, G.B.D.O., *Global, regional, and national burden of osteoarthritis, 1990-2020 and projections to 2050: a systematic analysis for the Global Burden of Disease Study 2021.* Lancet Rheumatol, 2023. **5**(9): p. e508-e522.

2. Centers for Disease, C. and Prevention, *Prevalence of doctor-diagnosed arthritis and arthritis-attributable activity limitation --- United States, 2007-2009.* MMWR Morb Mortal Wkly Rep, 2010. **59**(39): p. 1261-5.

3. Clinic, T.M. *Osteoarthritis*. Available from: https://www.mayoclinic.org/diseases-conditions/osteoarthritis/diagnosis-treatment/drc-20351930.

4. Tateiwa, D., H. Yoshikawa, and T. Kaito, *Cartilage and Bone Destruction in Arthritis: Pathogenesis and Treatment Strategy: A Literature Review.* Cells, 2019. **8**(8).

5. Sophia Fox, A.J., A. Bedi, and S.A. Rodeo, *The basic science of articular cartilage: structure, composition, and function.* Sports Health, 2009. **1**(6): p. 461-8.

6. Ohno, S., et al., *Expression of superficial zone protein in mandibular condyle cartilage.* Osteoarthritis Cartilage, 2006. **14**(8): p. 807-13.

7. Weis, M.A., et al., *Location of 3-hydroxyproline residues in collagen types I, II, III, and V/XI implies a role in fibril supramolecular assembly.* J Biol Chem, 2010. **285**(4): p. 2580-90.

8. O'Donnell, P. *Collagen*. [website] 2021 June 17 2021 [cited 2025 10/4/25].

9. Poole, C.A., M.H. Flint, and B.W. Beaumont, *Chondrons in cartilage: ultrastructural analysis of the pericellular microenvironment in adult human articular cartilages.* J Orthop Res, 1987. **5**(4): p. 509-22.

10. Chery, D.R., et al., *Early changes in cartilage pericellular matrix micromechanobiology portend the onset of post-traumatic osteoarthritis.* Acta Biomater, 2020. **111**: p. 267-278.

11. Quinn, T.M., et al., *Physical and biological regulation of proteoglycan turnover around chondrocytes in cartilage explants. Implications for tissue degradation and repair.* Ann N Y Acad Sci, 1999. **878**: p. 420-41.

12. Shah, S.S. and K. Mithoefer, *Scientific Developments and Clinical Applications Utilizing Chondrons and Chondrocytes with Matrix for Cartilage Repair.* Cartilage, 2021. **13**(1_suppl): p. 1195S-1205S.

13. Muir, H., *The chondrocyte, architect of cartilage. Biomechanics, structure, function and molecular biology of cartilage matrix macromolecules.* Bioessays, 1995. **17**(12): p. 1039-48.

14. Goldring, M.B. and S.R. Goldring, *Articular cartilage and subchondral bone in the pathogenesis of osteoarthritis.* Ann N Y Acad Sci, 2010. **1192**: p. 230-7.

15. Hunter, D.J. and S. Bierma-Zeinstra, *Osteoarthritis.* Lancet, 2019. **393**(10182): p. 1745-1759.

16. Zhao, Z., et al., *Mechanotransduction pathways in the regulation of cartilage chondrocyte homoeostasis.* J Cell Mol Med, 2020. **24**(10): p. 5408-5419.

17. Di, X., et al., *Cellular mechanotransduction in health and diseases: from molecular mechanism to therapeutic targets.* Signal Transduct Target Ther, 2023. **8**(1): p. 282.

18. Zheng, L., et al., *The role of metabolism in chondrocyte dysfunction and the progression of osteoarthritis.* Ageing Res Rev, 2021. **66**: p. 101249.

19. Adam, M.S., et al., *The metabolic characteristics and changes of chondrocytes in vivo and in vitro in osteoarthritis.* Front Endocrinol (Lausanne), 2024. **15**: p. 1393550.

20. Ansari, M.Y., N. Ahmad, and T.M. Haqqi, *Oxidative stress and inflammation in osteoarthritis pathogenesis: Role of polyphenols.* Biomed Pharmacother, 2020. **129**: p. 110452.

21. Arjun, A., et al., *Metabolomics in Osteoarthritis Knee: A Systematic Review of Literature.* Indian J Orthop, 2024. **58**(7): p. 813-828.

22. Lei, Z., D.V. Huhman, and L.W. Sumner, *Mass spectrometry strategies in metabolomics.* J Biol Chem, 2011. **286**(29): p. 25435-42.

23. Lee, D.Y., B.P. Bowen, and T.R. Northen, *Mass spectrometry-based metabolomics, analysis of metabolite-protein interactions, and imaging.* Biotechniques, 2010. **49**(2): p. 557-65.

24. *Osteoarthritis Action Alliance*. OA Pathogenesis and Risk Factors [cited 2025 10/4].

25. Adhitya, I., et al., *The Risk Factors and Preventive Strategies of Poor Knee Functions and Osteoarthritis after Anterior Cruciate Ligament Reconstruction: A Narrative Review.* Phys Ther Res, 2023. **26**(3): p. 78-88.

26. Riewruja, K., et al., *Experimental models to study osteoarthritis pain and develop therapeutics.* Osteoarthr Cartil Open, 2022. **4**(4): p. 100306.

27. Patwari, P., *Proteoglyan Degradation After Injurious Compression of Bovine and Human Articular Cartilage In Vitro.* Arthritis & Rheumatism, 2003.

28. Quinn, T.M., et al., *Effects of injurious compression on matrix turnover around individual cells in calf articular cartilage explants.* J Orthop Res, 1998. **16**(4): p. 490-9.

29. Rocssncr, U. and J. Bownel, *What is metabolomics all about?* BioTechniques, 2009.

30. Brahmachary, P.P., H.D. Welhaven, and R.K. June, *Metabolomic Profiling to Understand Chondrocyte Metabolism.* Methods Mol Biol, 2023. **2598**: p. 141-156.

31. Nims, R.J., et al., *Synthesis rates and binding kinetics of matrix products in engineered cartilage constructs using chondrocyte-seeded agarose gels.* J Biomech, 2014. **47**(9): p. 2165-72.

32. Jutila, A.A., et al., *Encapsulation of chondrocytes in high-stiffness agarose microenvironments for in vitro modeling of osteoarthritis mechanotransduction.* Ann Biomed Eng, 2015. **43**(5): p. 1132-44.

33. Sengprasert, P., et al., *The Immunological Facets Of Chondrocytes In Osteoarthritis: A Narrative Review.* J Rheumatol, 2023.

34. Song, Y., Z. Wu, and P. Zhao, *The effects of metformin in the treatment of osteoarthritis: Current perspectives.* Front Pharmacol, 2022. **13**: p. 952560.

35. Lee, J., et al., *Metformin Induces Apoptosis and Inhibits Proliferation through the AMP-Activated Protein Kinase and Insulin-like Growth Factor 1 Receptor Pathways in the Bile Duct Cancer Cells.* J Cancer, 2019. **10**(7): p. 1734-1744.

36. Schmidt, M.M. and R. Dringen, *Differential effects of iodoacetamide and iodoacetate on glycolysis and glutathione metabolism of cultured astrocytes.* Front Neuroenergetics, 2009. **1**: p. 1.

37. Jiang, L., et al., *Monosodium iodoacetate induces apoptosis via the mitochondrial pathway involving ROS production and caspase activation in rat chondrocytes in vitro.* J Orthop Res, 2013. **31**(3): p. 364-9.

38. Pitcher, T., J. Sousa-Valente, and M. Malcangio, *The Monoiodoacetate Model of Osteoarthritis Pain in the Mouse.* J Vis Exp, 2016(111).

39. Christiansen, B.A., et al., *Non-invasive mouse models of post-traumatic osteoarthritis.* Osteoarthritis Cartilage, 2015. **23**(10): p. 1627-38.

40. Øiestad, B.E., *Knee Osteoarthritis After Anterior Cruciate Ligament Injury.* The American Journal of Sports Medicine, 2008.

41. Juneja, P., A. Munjal, and J.B. Hubbard, *Anatomy, Joints*, in *StatPearls*. 2024: Treasure Island (FL).

42. Kurz, B., et al., *Influence of tissue maturation and antioxidants on the apoptotic response of articular cartilage after injurious compression.* Arthritis Rheum, 2004. **50**(1): p. 123-30.

43. Henrotin, Y., B. Kurz, and T. Aigner, *Oxygen and reactive oxygen species in cartilage degradation: friends or foes?* Osteoarthritis Cartilage, 2005. **13**(8): p. 643-54.

44. Sandell, L.J. and T. Aigner, *Articular cartilage and changes in arthritis. An introduction: cell biology of osteoarthritis.* Arthritis Res, 2001. **3**(2): p. 107-13.

45. Goldring, S.R. and M.B. Goldring, *The role of cytokines in cartilage matrix degeneration in osteoarthritis.* Clin Orthop Relat Res, 2004(427 Suppl): p. S27-36.

46. Pi, P., et al., *The role of targeting glucose metabolism in chondrocytes in the pathogenesis and therapeutic mechanisms of osteoarthritis: a narrative review.* Front Endocrinol (Lausanne), 2024. **15**: p. 1319827.

47. Brahmachary, P.P., *Metabolomic Profiling to Understand Chondrocyte Metabolism.* 2023.

48. Mobasheri, A., et al., *The role of metabolism in the pathogenesis of osteoarthritis.* Nat Rev Rheumatol, 2017. **13**(5): p. 302-311.

49. Maneiro, E., et al., *Mitochondrial respiratory activity is altered in osteoarthritic human articular chondrocytes.* Arthritis Rheum, 2003. **48**(3): p. 700-8.

50. Rajpurohit, R., et al., *Adaptation of chondrocytes to low oxygen tension: relationship between hypoxia and cellular metabolism.* J Cell Physiol, 1996. **168**(2): p. 424-32.

51. Cheung, C., et al., *Mitochondrial quality control dysfunction in osteoarthritis: Mechanisms, therapeutic strategies & future prospects.* Arch Gerontol Geriatr, 2024. **125**: p. 105522.

52. Chinopoulos, C., *OXPHOS Defects Due to mtDNA Mutations: Glutamine to the Rescue!* Cell Metab, 2018. **27**(6): p. 1165-1167.

APPENDICES

APPENDIX A

METABOLITES OF INTEREST (INJURY CAUSES ALTERED METABOLISM AND OXYGEN CONSUMPTION)

Supplemental Table 1: Metabolites of Interest

Metabolite	**Pathway**
Pyruvic Acid	Glycolysis
Lactic Acid	Anerobic Glycolysis
Fumaric Acid	TCA
Succinic Acid	TCA
Oxaloacetic Acid	TCA
Malic Acid	TCA
Alpha-ketoglutarate:2-oxogularic acid	TCA
Glutamine	TCA precursor, Amino Acid precursor
Glutamic Acid	TCA precursor, Amino Acid precursor
Phosphoenolpyruvate: phosphoenol pyruvic acid	Glycolysis
Fructose/Glucose	Glycolysis
Citric Acid	TCA
Fructose 6 phosphate	Glycolysis
6-phospho-gluconate	PPP
Sedoheptulose-7-phosphate	PPP
NADH	Glycolysis or TCA
HS-CoA	TCA

APPENDIX B

HEATMAPS OF NON TII CORRECTED METABOLITE

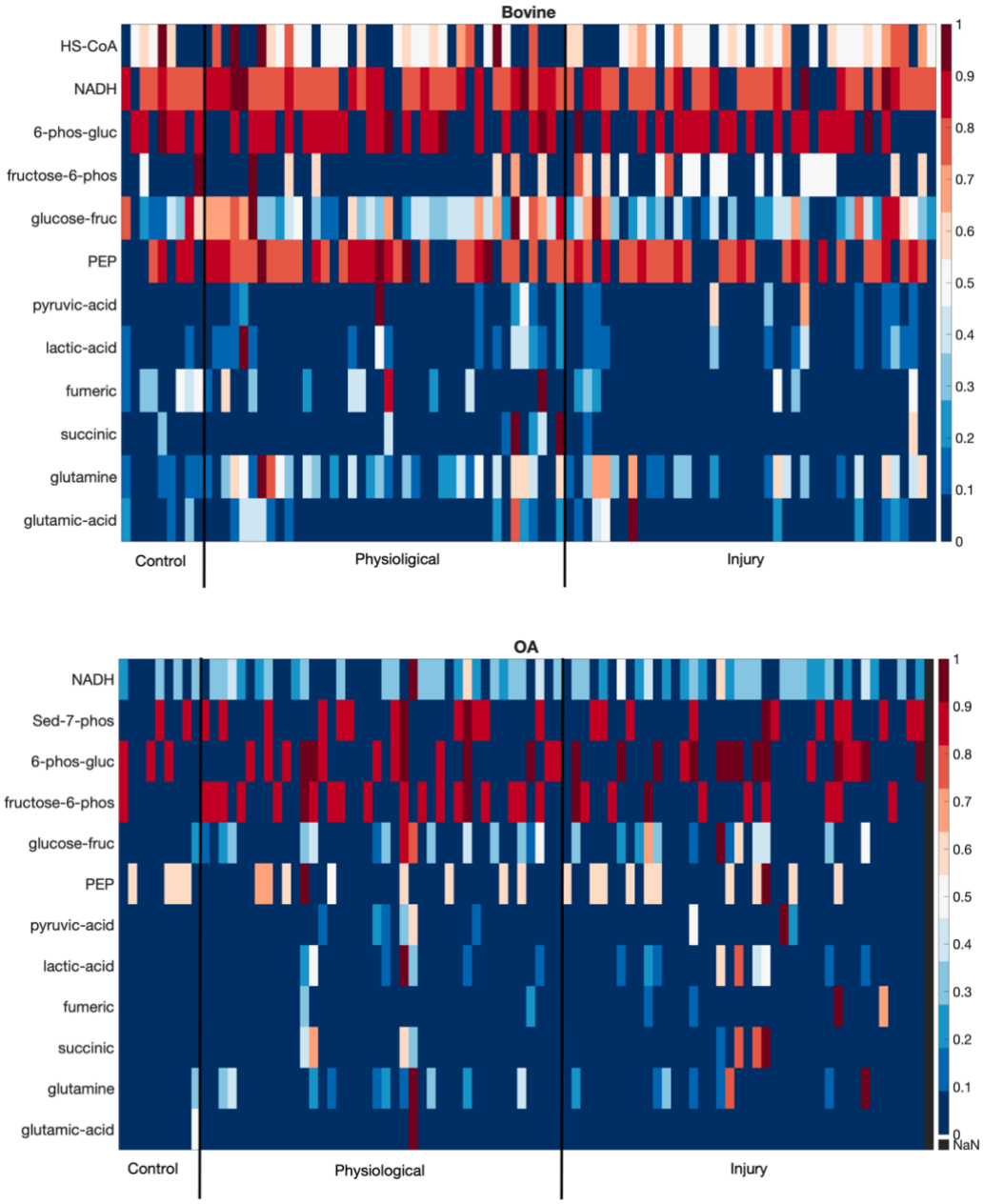

Supplemental Figure 1: Metabolite Concentration represented as a set of the total. Control, physiological, and injury loading condition with the detected metabolites, neither the metabolites or the samples are clustered. Panel A shows bovine chondrocytes and panel B shows OA chondrocytes.

APPENDIX C

HEAT MAPS OF TII CORRECTED METABOLITES SHOWN IN GROUPS

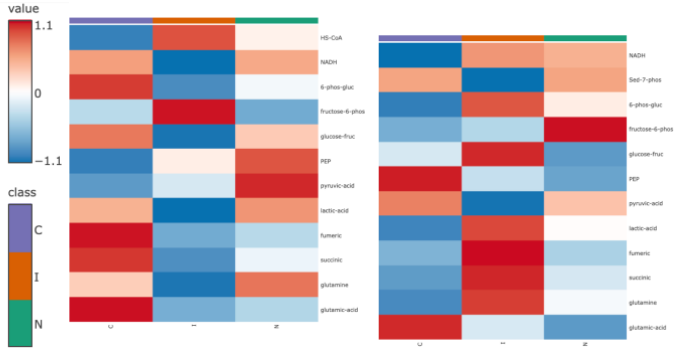

Supplemental Figure 2: TIC corrected Average metabolite concentration per loading group scaled to a range of 1.1 to -1.1. A: OA donors, C = control, I = injury, N = normal. B: Bovine samples, C = control, I = injury, N = normal. The y axis shows the detected metabolites of interest.

APPENDIX D

OA STATISTICAL TEST: LABEL EFFECT AND TIME EFFECT. ONLY SHOWN IF FALLEN INTO THE PROPER AS DESCRIBED IN CHAPTER 3.

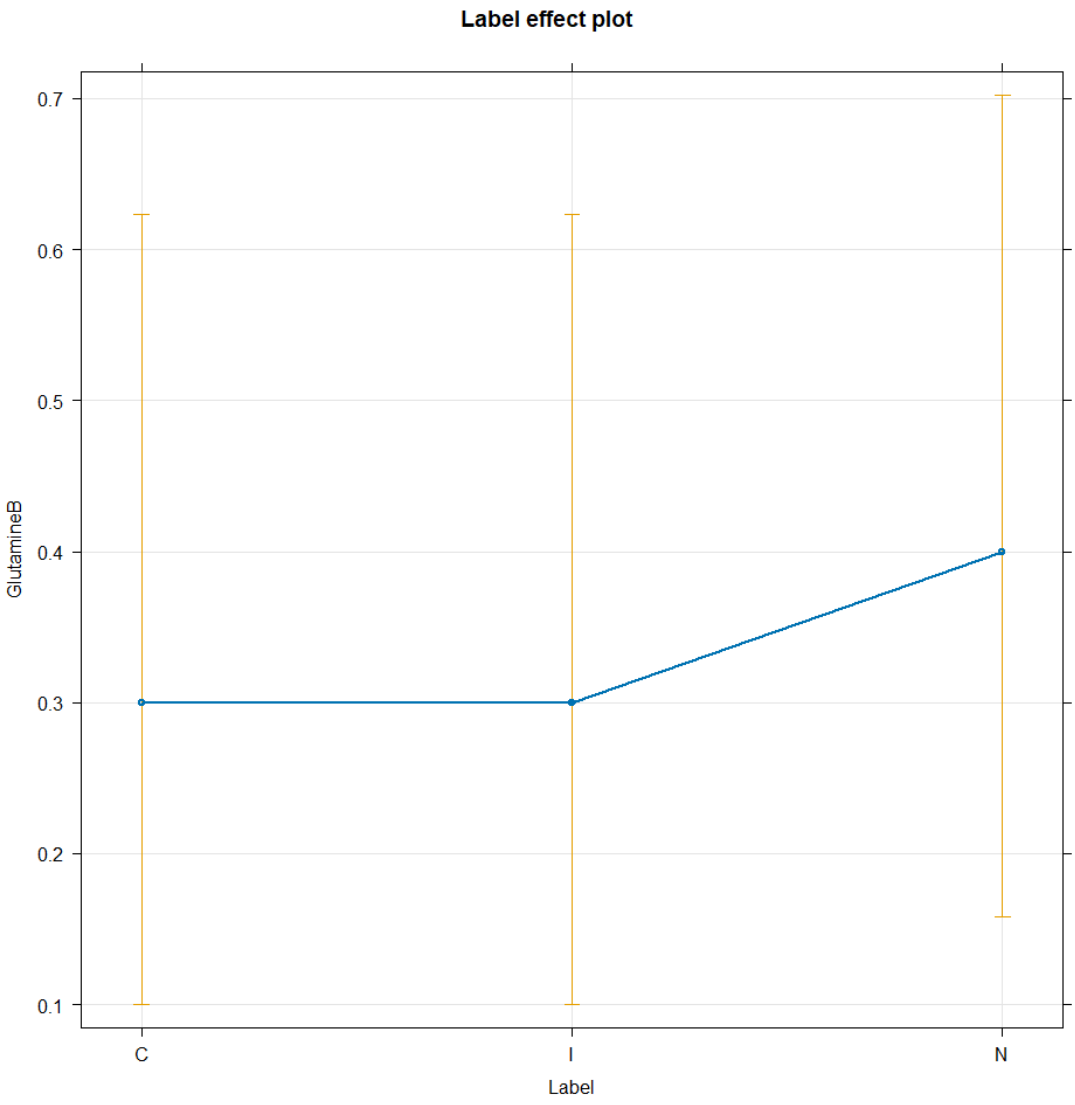
Label effect plot
GlutamineB
0.7
0.6
0.5
0.4
0.3
0.2
0.1
C
I
N
Label

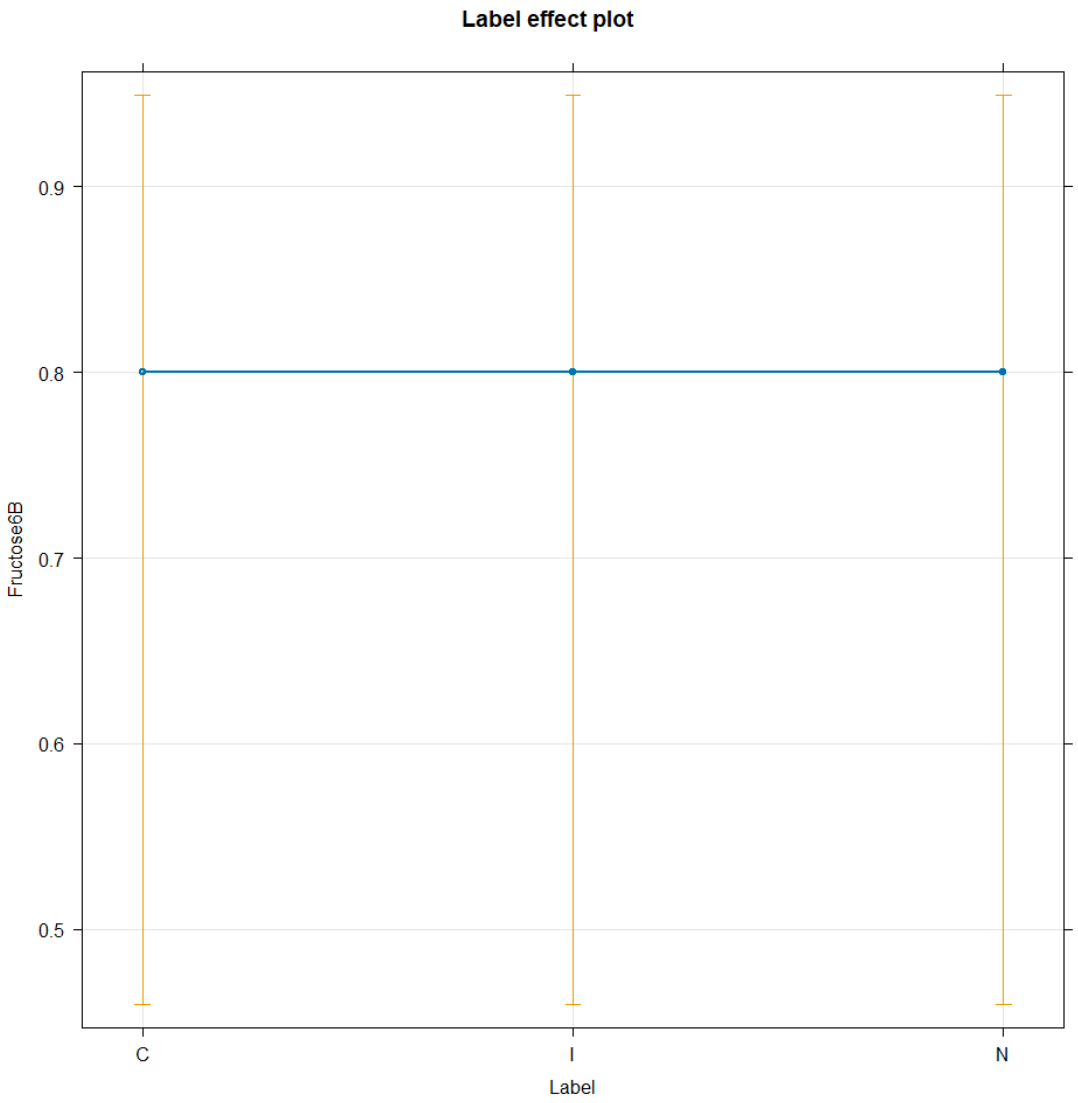
Label effect plot
Fructose6B
0.9
0.8
0.7
0.6
0.5
C
I
N
Label

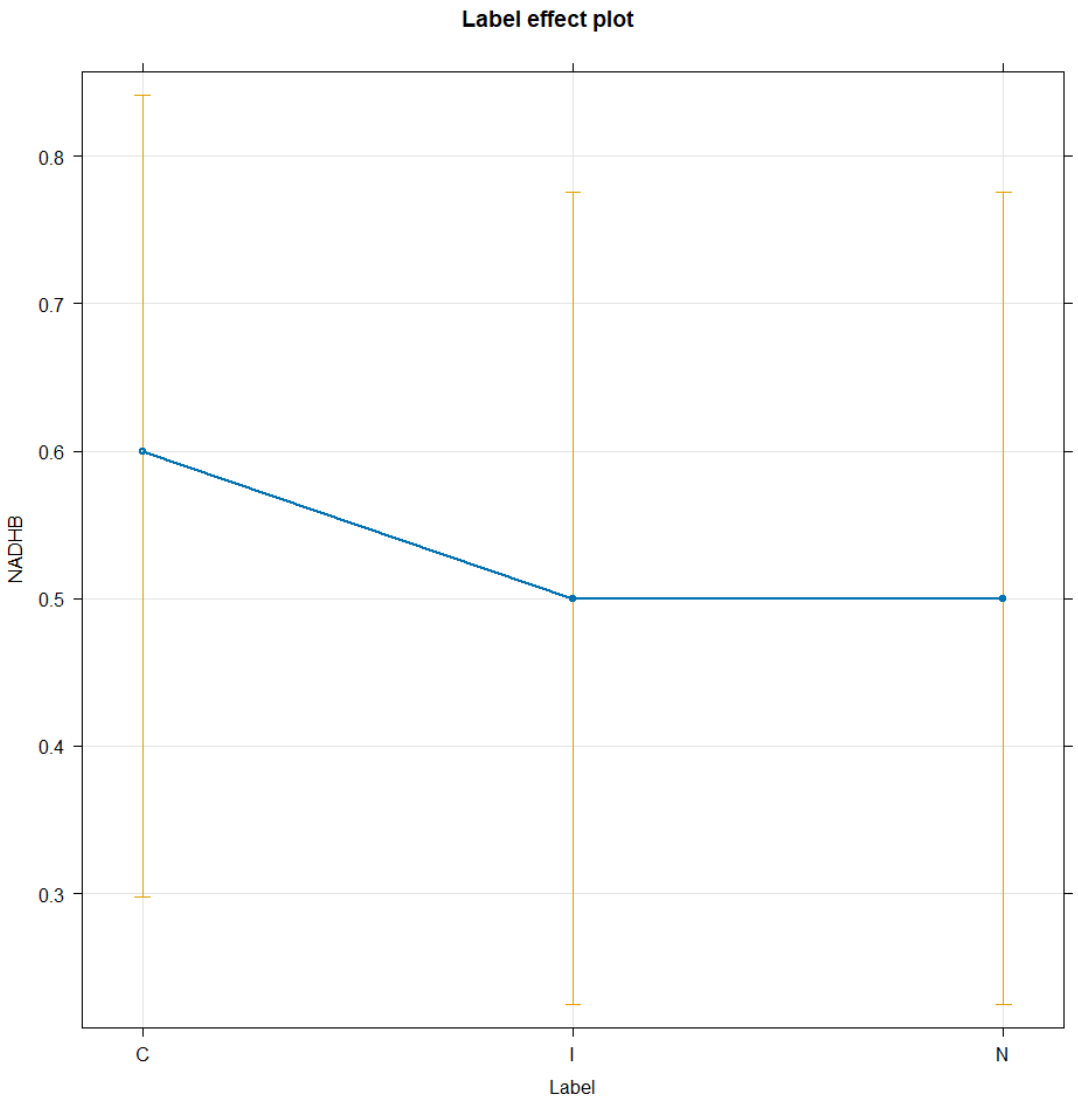
Label effect plot
NADHB
0.8
0.7
0.6
0.5
0.4
0.3
C
I
N
Label

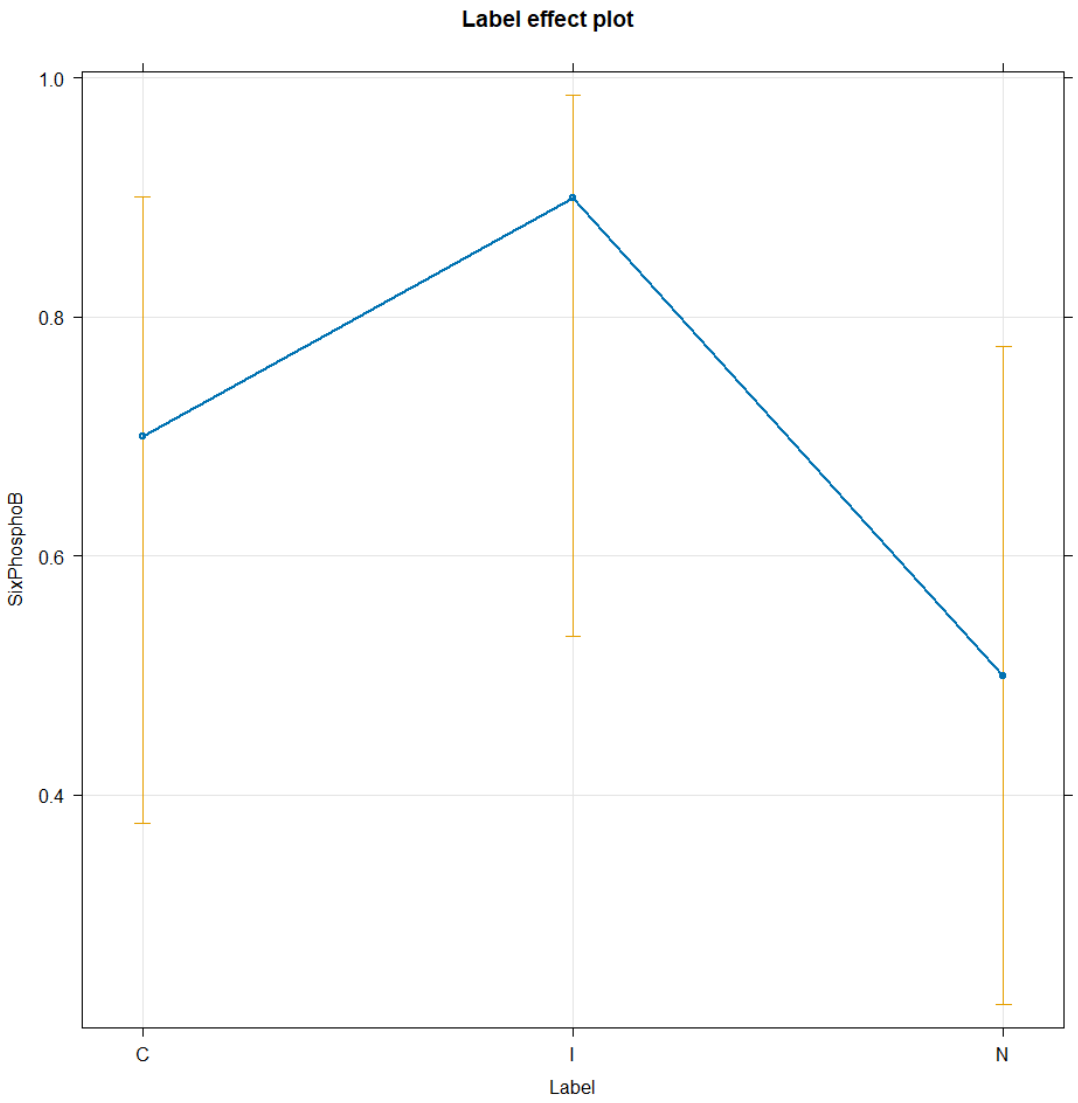
Label effect plot
1.0
0.8
0.6
0.4
SixPhosphoB
C
I
N
Label

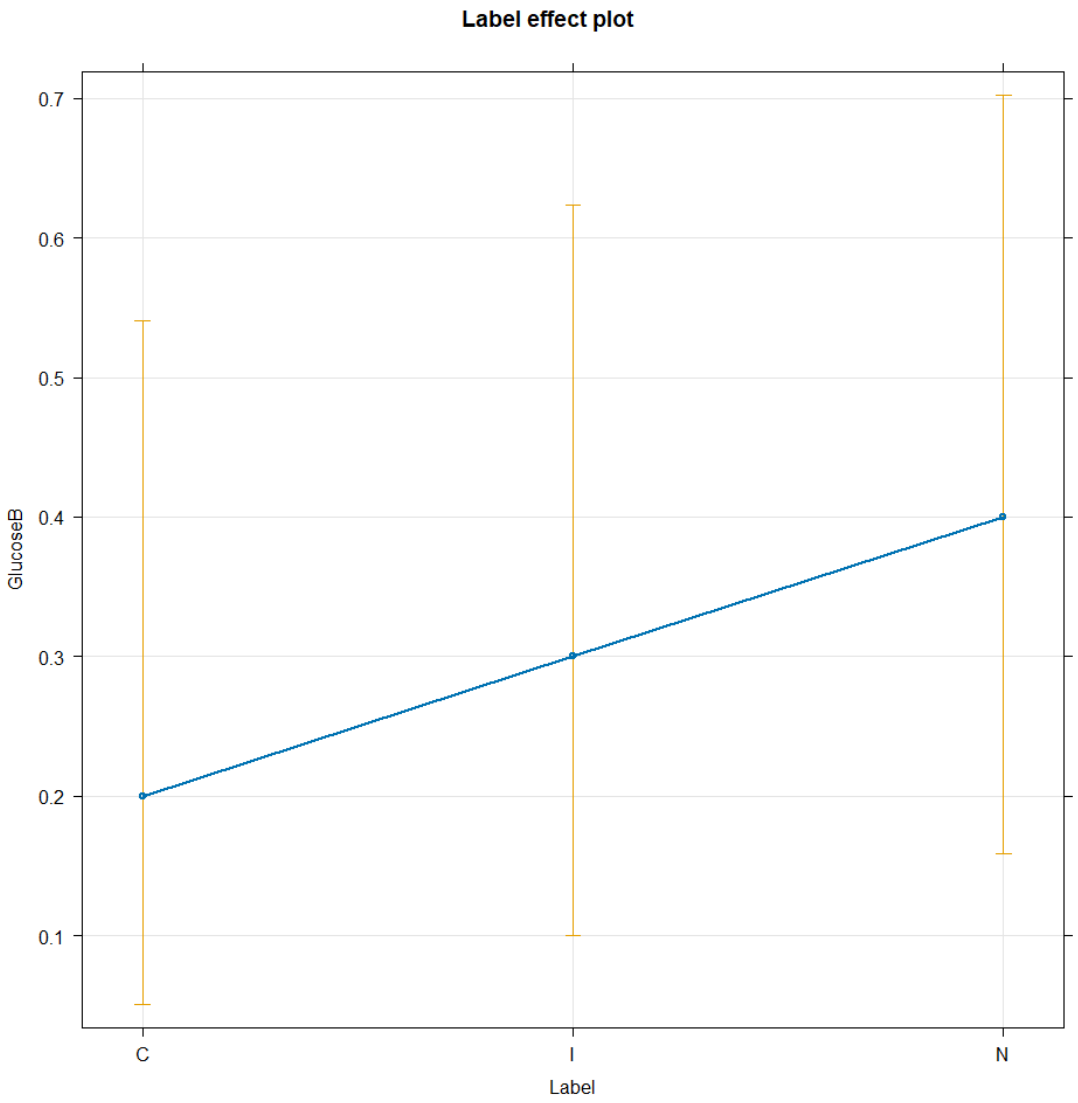
Label effect plot
GlucoseB
0.7
0.6
0.5
0.4
0.3
0.2
0.1
C
I
N
Label

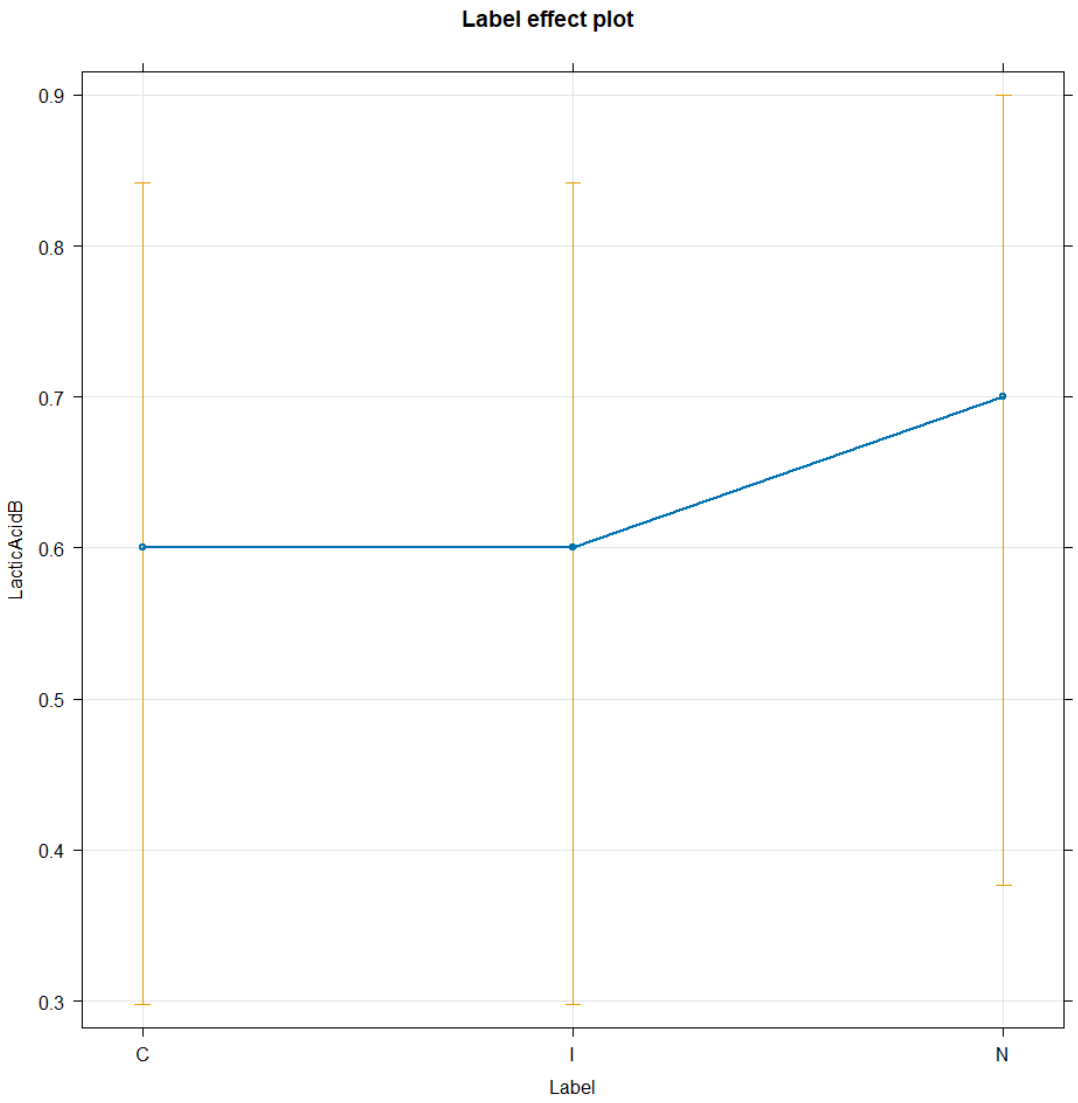
Label effect plot
LacticAcidB
0.9
0.8
0.7
0.6
0.5
0.4
0.3
C
I
N
Label

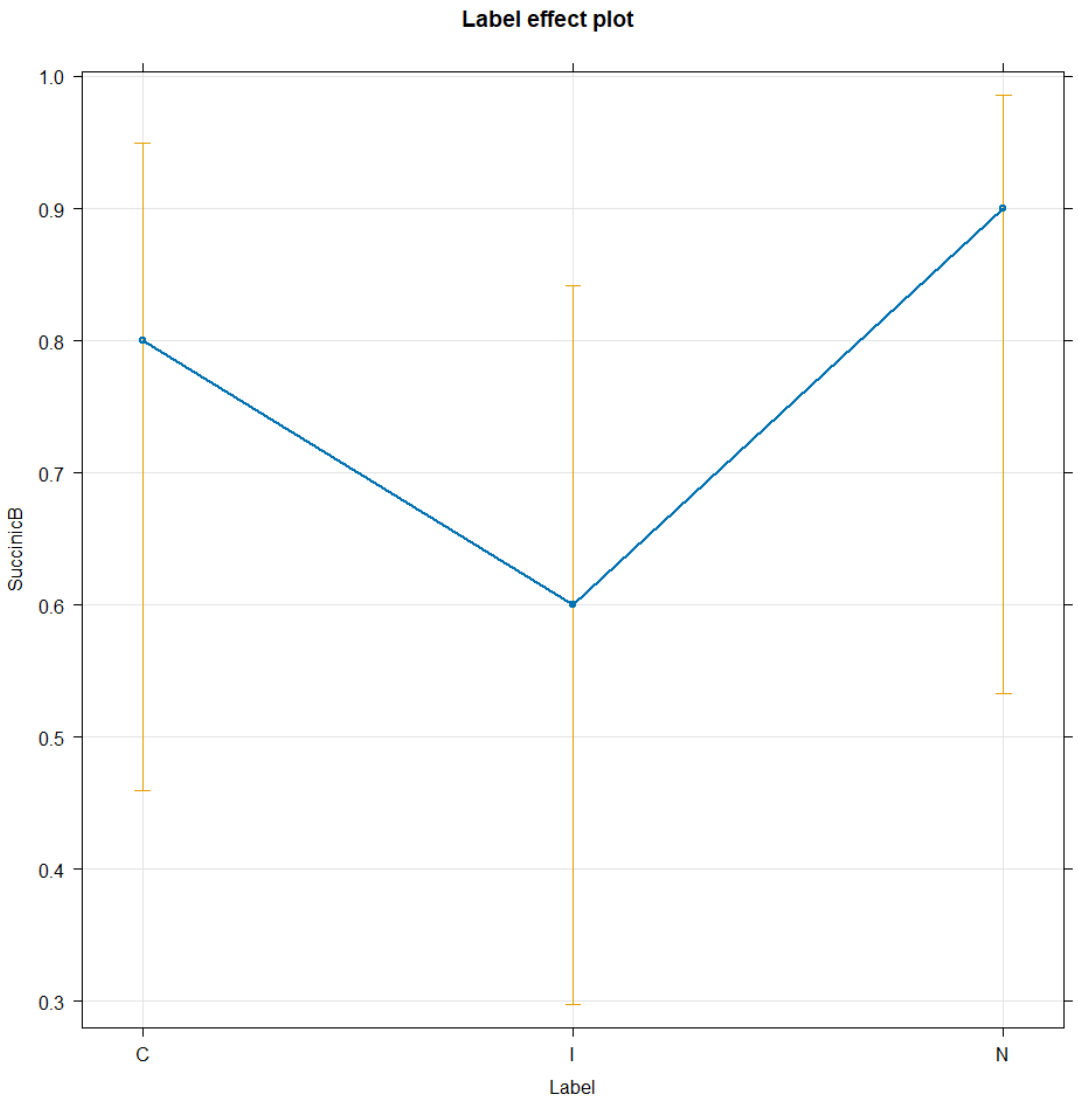
Label effect plot
1.0
0.9
0.8
0.7
0.6
0.5
0.4
0.3
SuccinicB
C
I
N
Label

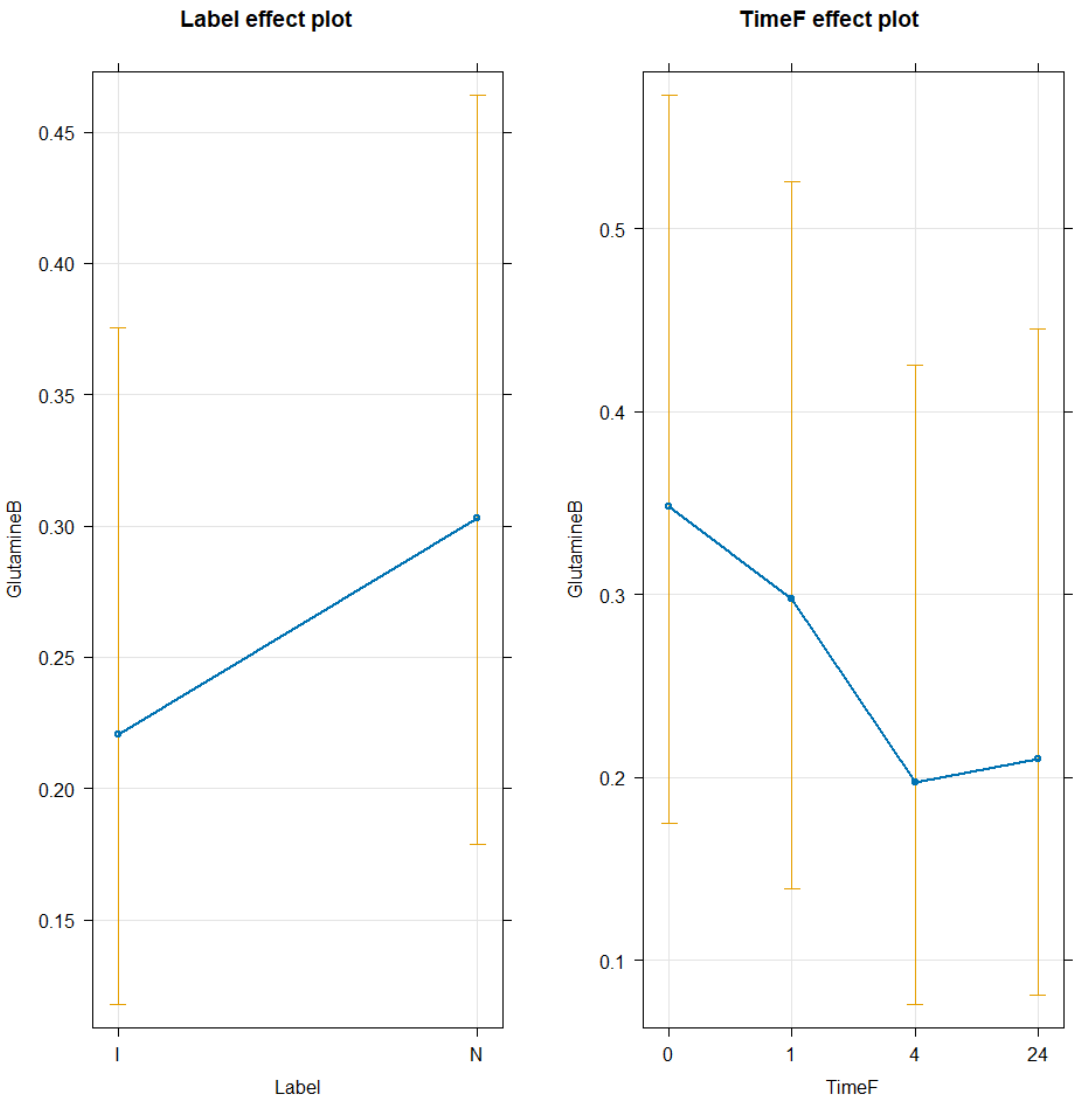
Label effect plot
GlutamineB
0.45
0.40
0.35
0.30
0.25
0.20
0.15
I
N
Label
TimeF effect plot
GlutamineB
0.5
0.4
0.3
0.2
0.1
0
1
4
24
TimeF

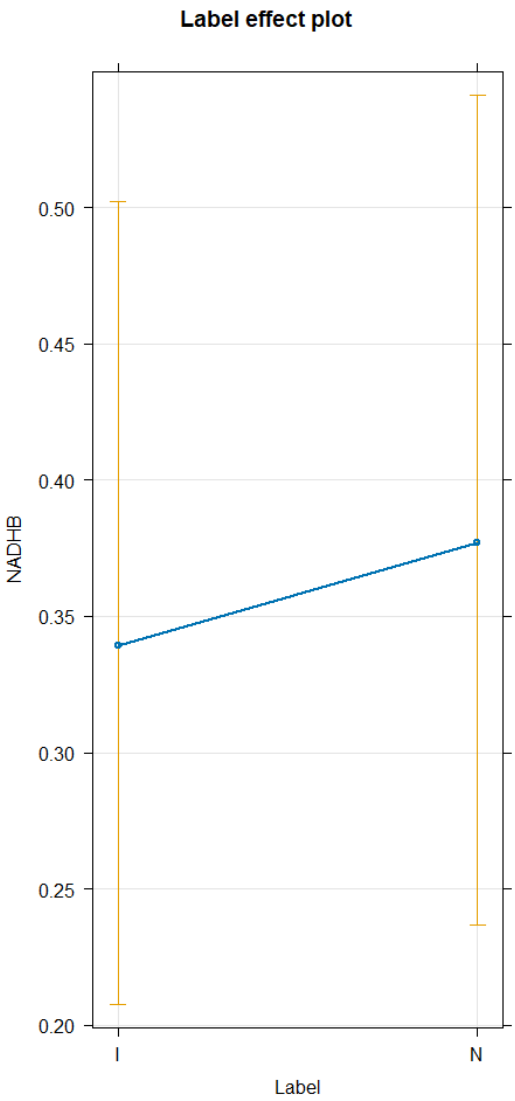
Label effect plot
NADHB
0.50
0.45
0.40
0.35
0.30
0.25
0.20
I
N
Label

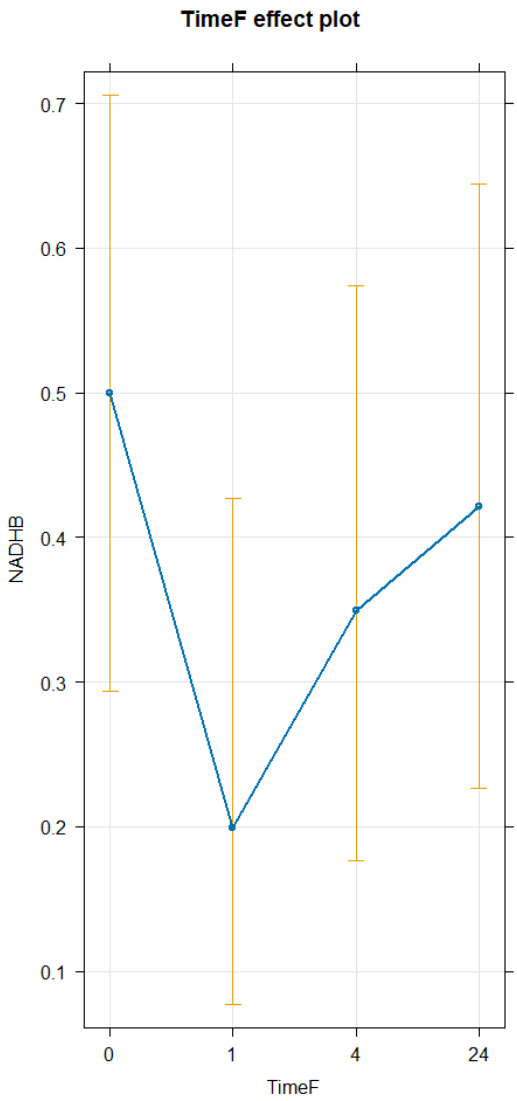
TimeF effect plot
NADHB
0.7
0.6
0.5
0.4
0.3
0.2
0.1
0
1
4
24
TimeF

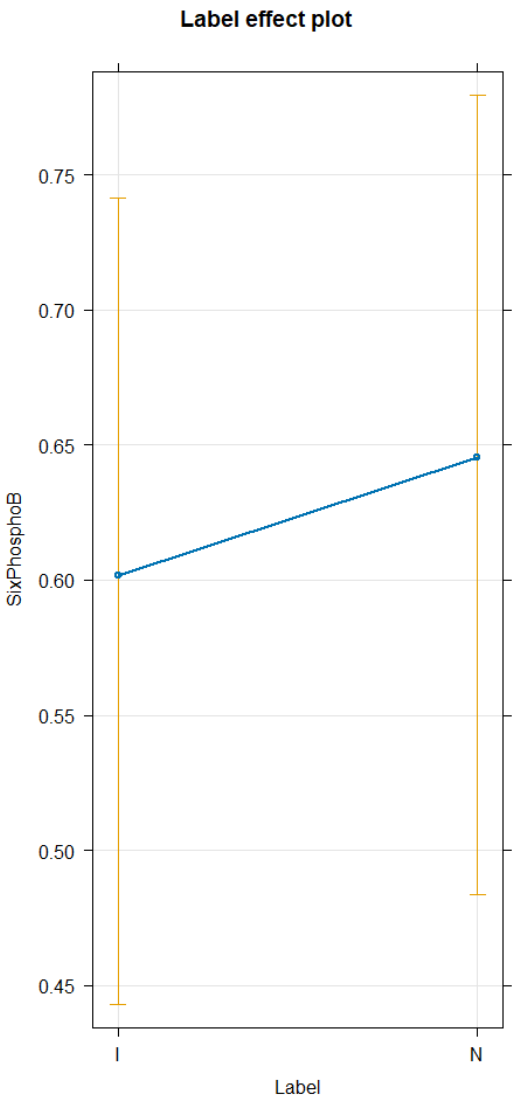
Label effect plot
SixPhosphoB
0.75
0.70
0.65
0.60
0.55
0.50
0.45
I
N
Label

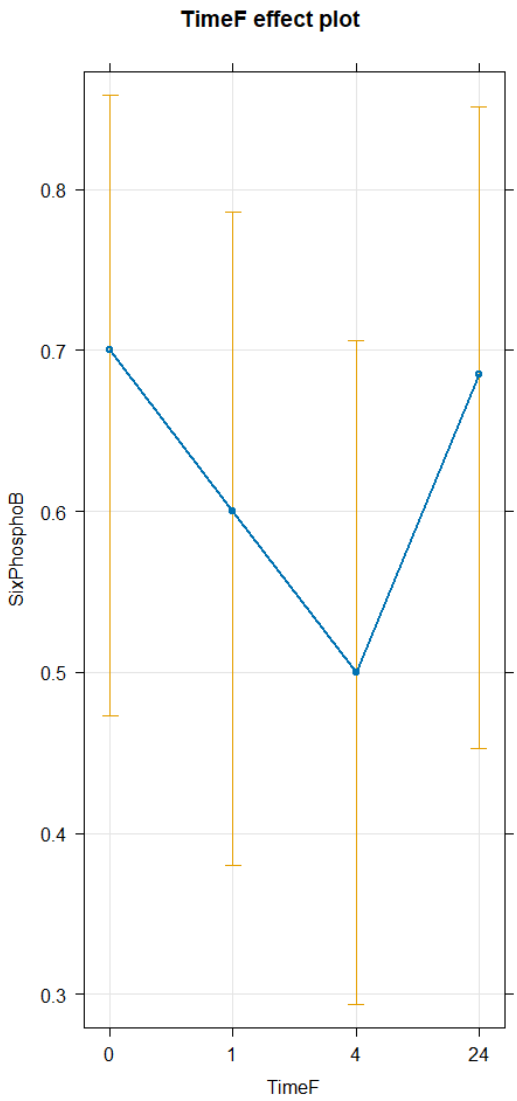
TimeF effect plot
SixPhosphoB
0.8
0.7
0.6
0.5
0.4
0.3
0
1
4
24
TimeF

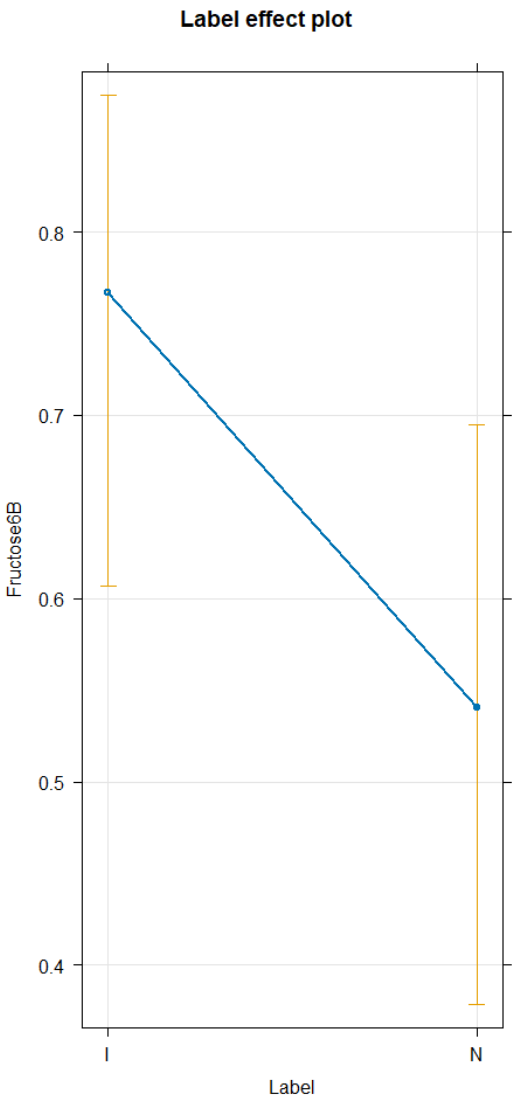
Label effect plot
Fructose6B
0.8
0.7
0.6
0.5
0.4
I
N
Label

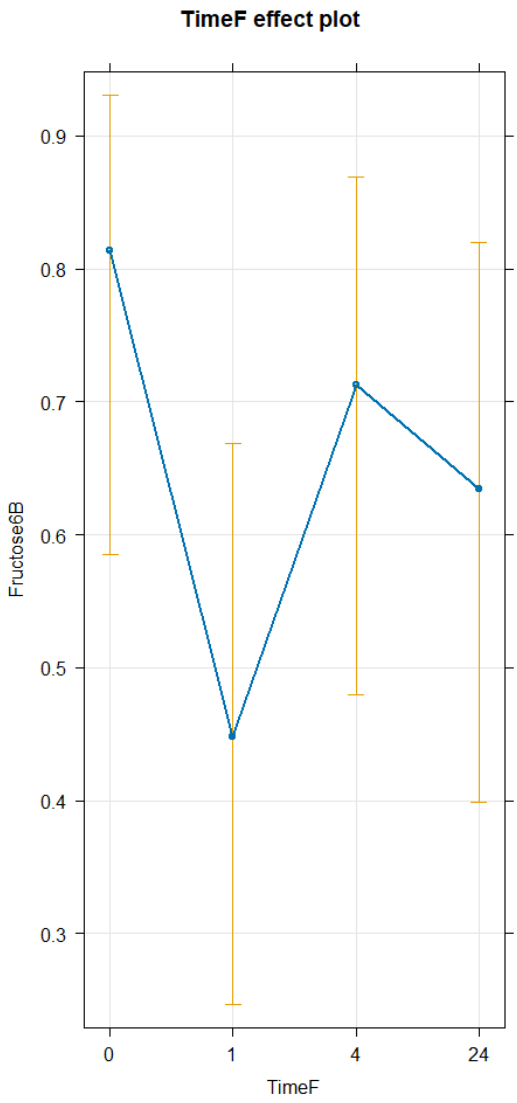
TimeF effect plot
Fructose6B
0.9
0.8
0.7
0.6
0.5
0.4
0.3
0
1
4
24
TimeF

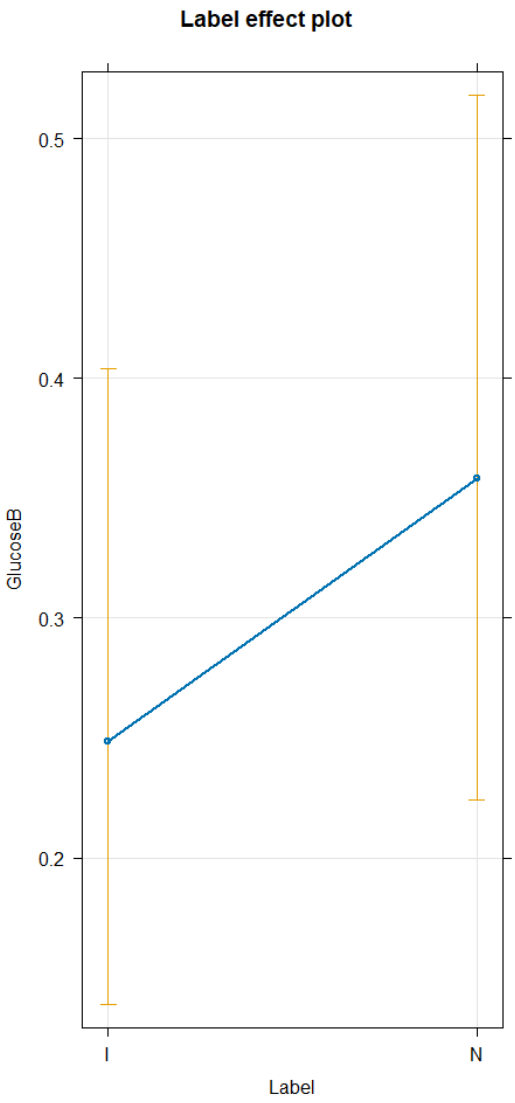
Label effect plot
GlucoseB
0.5
0.4
0.3
0.2
I
N
Label

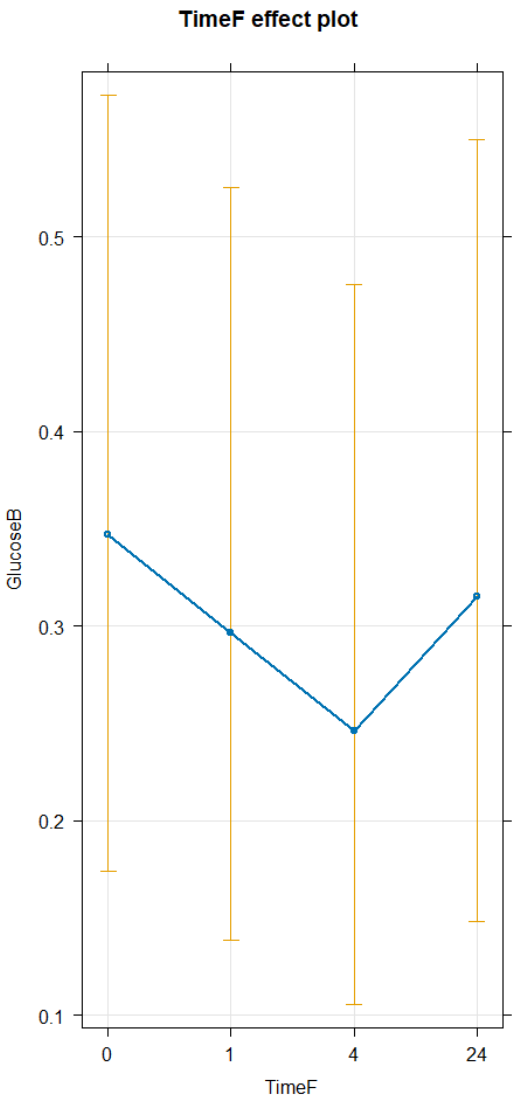
TimeF effect plot
GlucoseB
0.5
0.4
0.3
0.2
0.1
0
1
4
24
TimeF

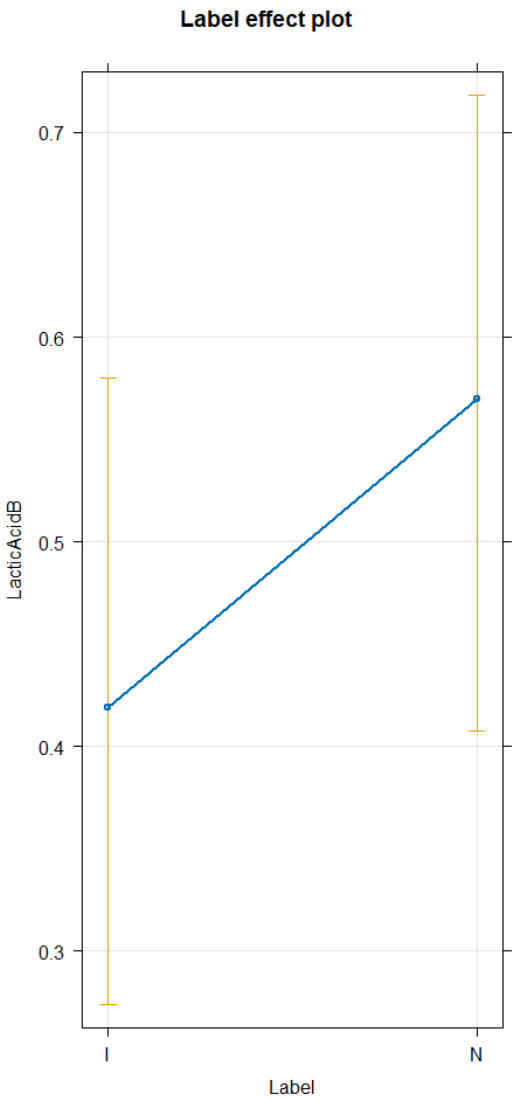
Label effect plot
LacticAcidB
0.7
0.6
0.5
0.4
0.3
I
N
Label

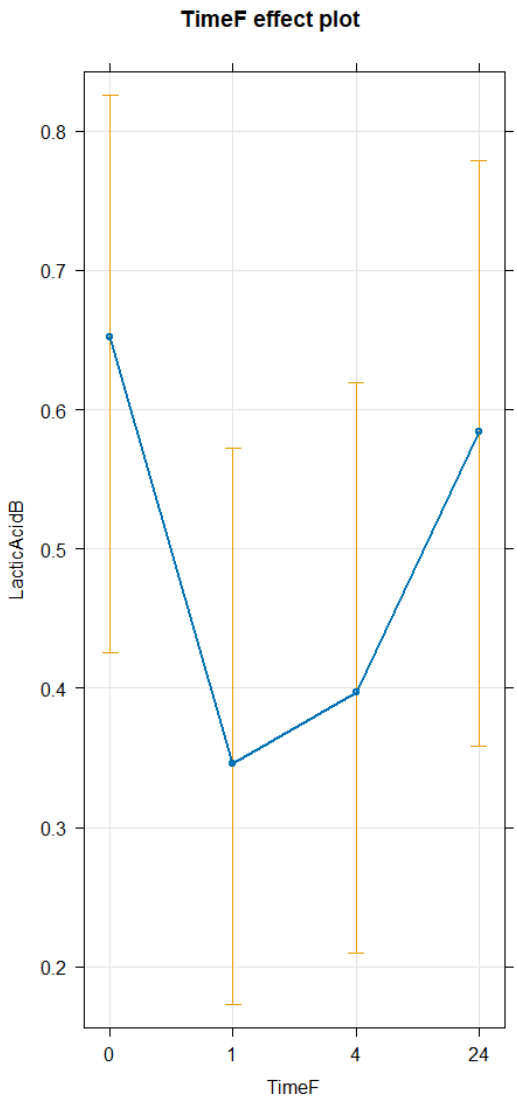
TimeF effect plot
LacticAcidB
0.8
0.7
0.6
0.5
0.4
0.3
0.2
0
1
4
24
TimeF

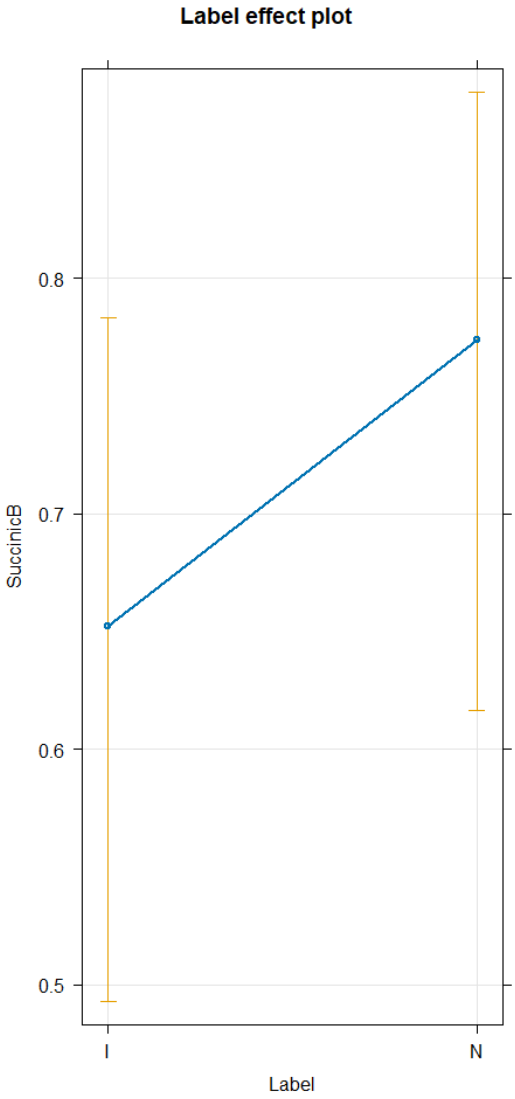
Label effect plot
SuccinicB
0.8
0.7
0.6
0.5
I
N
Label

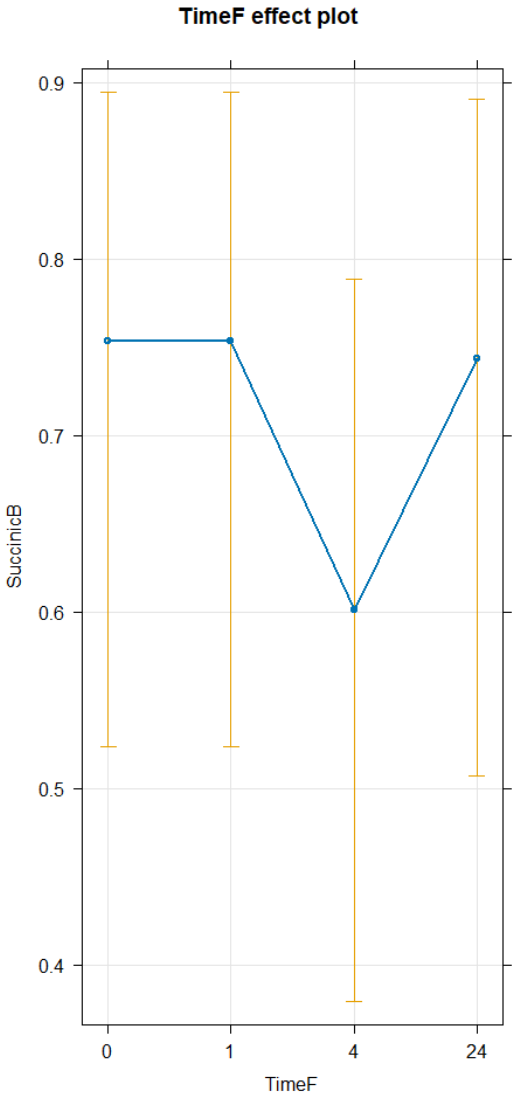
TimeF effect plot
SuccinicB
0.9
0.8
0.7
0.6
0.5
0.4
0
1
4
24
TimeF

APPENDIX D

BOVINE STATISTICAL TEST: LABEL EFFECT AND TIME EFFECT. ONLY SHOWN IF FALLEN INTO THE PROPER CATEGORIES AS DESCRIBED CHAPTER 3.

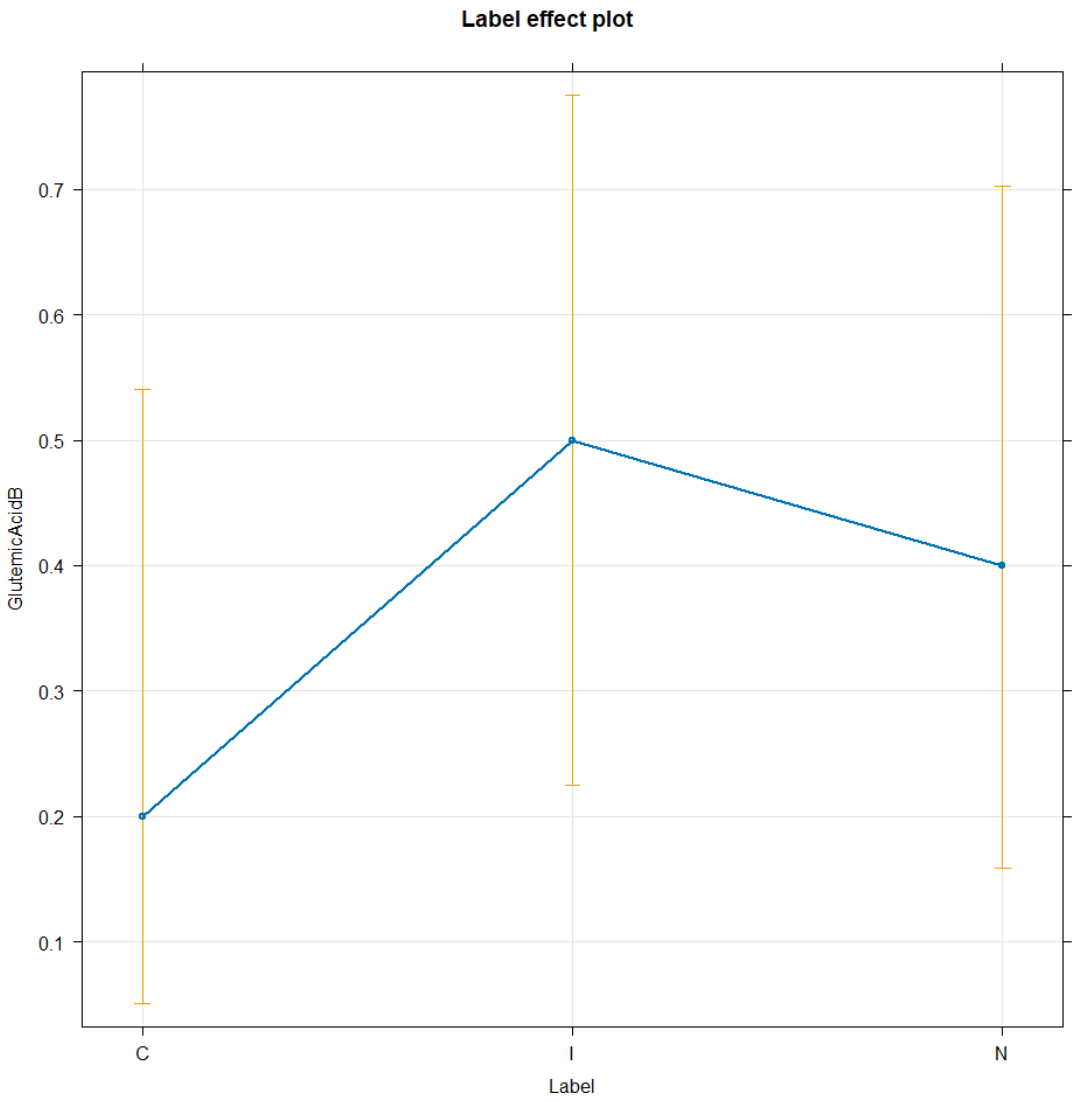
Label effect plot
GlutemicAcidB
0.7
0.6
0.5
0.4
0.3
0.2
0.1
C
I
N
Label

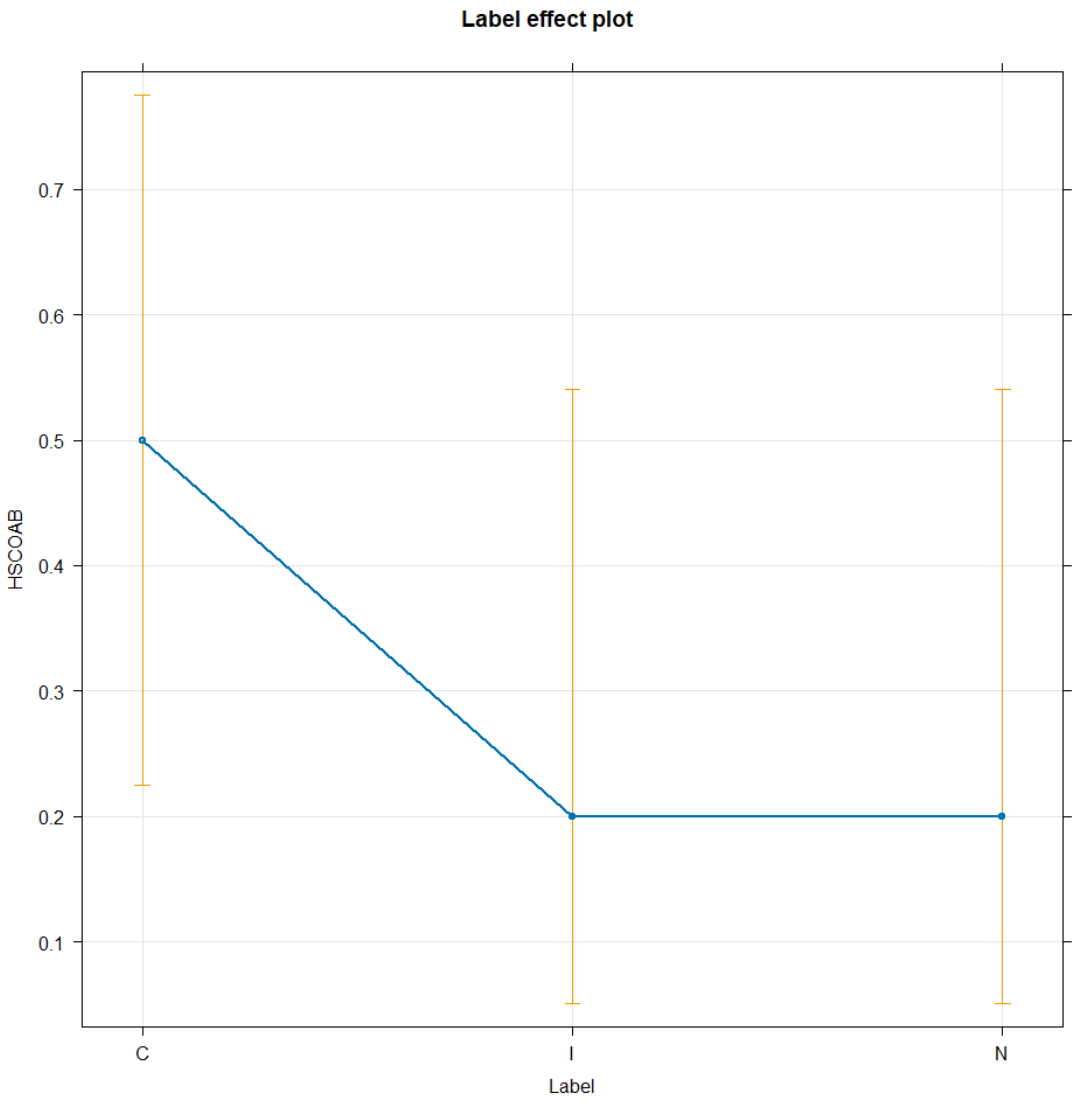
Label effect plot
HSCOAB
0.7
0.6
0.5
0.4
0.3
0.2
0.1
C
I
N
Label

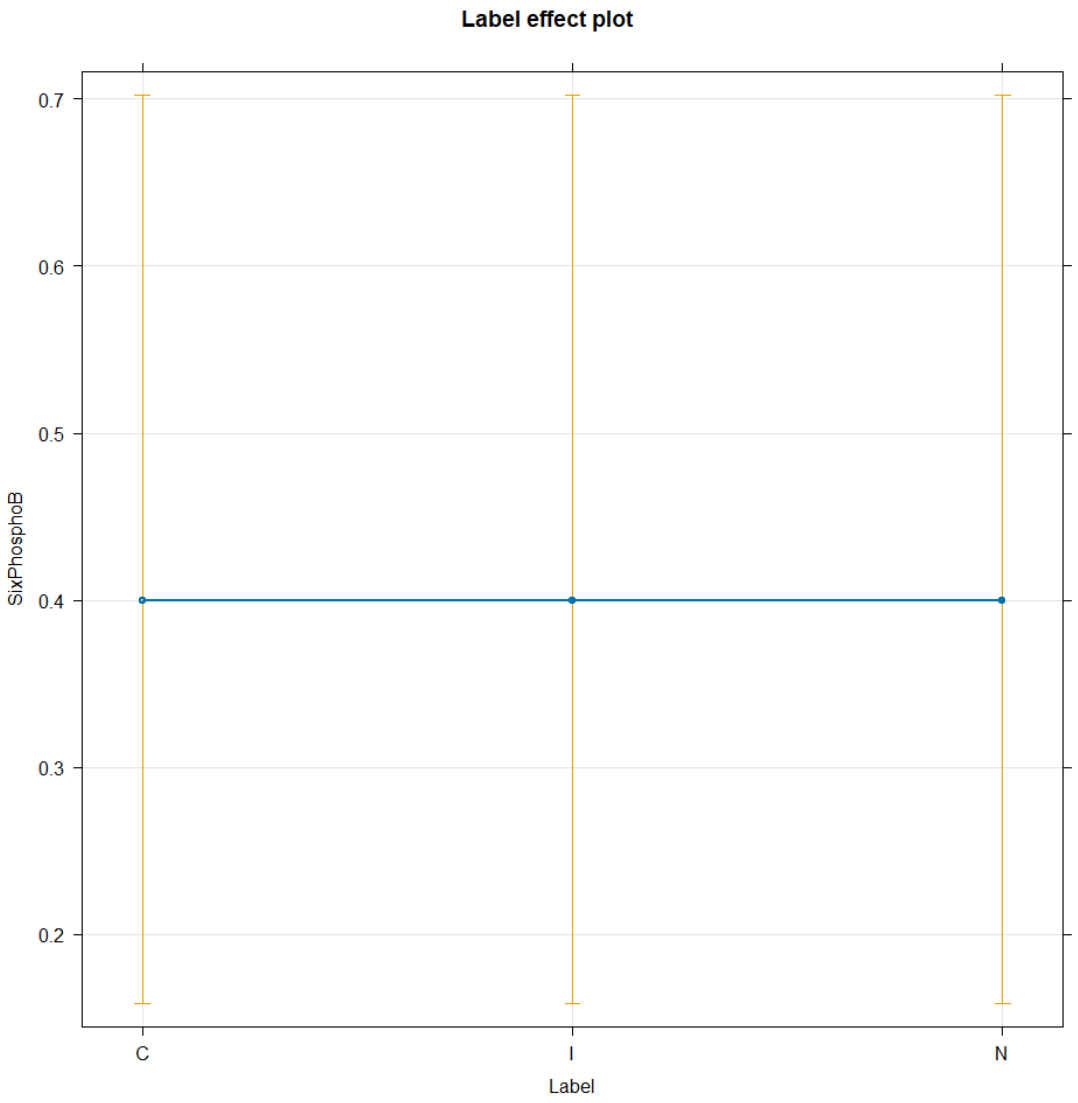
Label effect plot
SixPhosphoB
0.7
0.6
0.5
0.4
0.3
0.2
C
I
N
Label

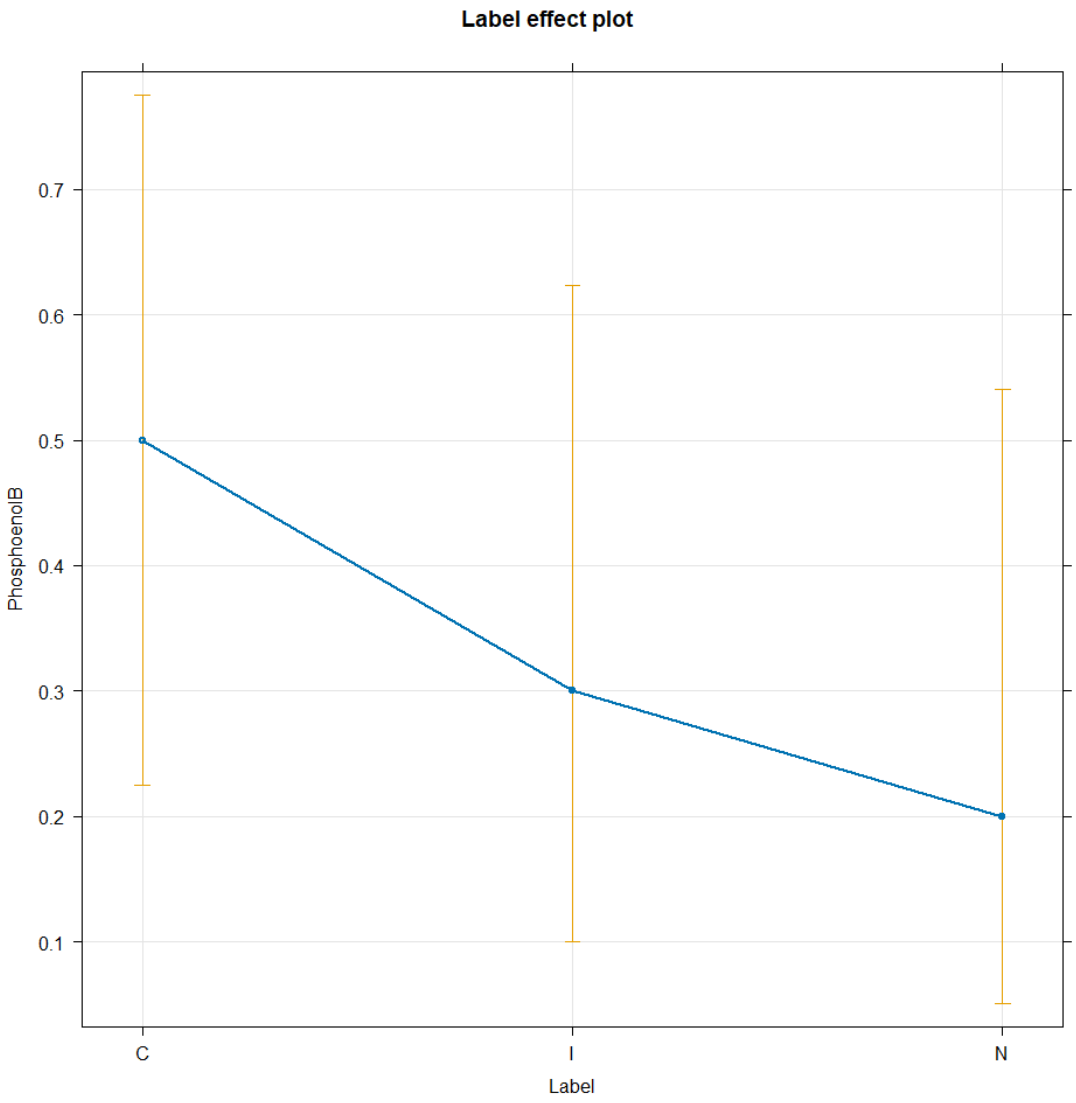
Label effect plot
PhosphoenolB
0.7
0.6
0.5
0.4
0.3
0.2
0.1
C
I
N
Label

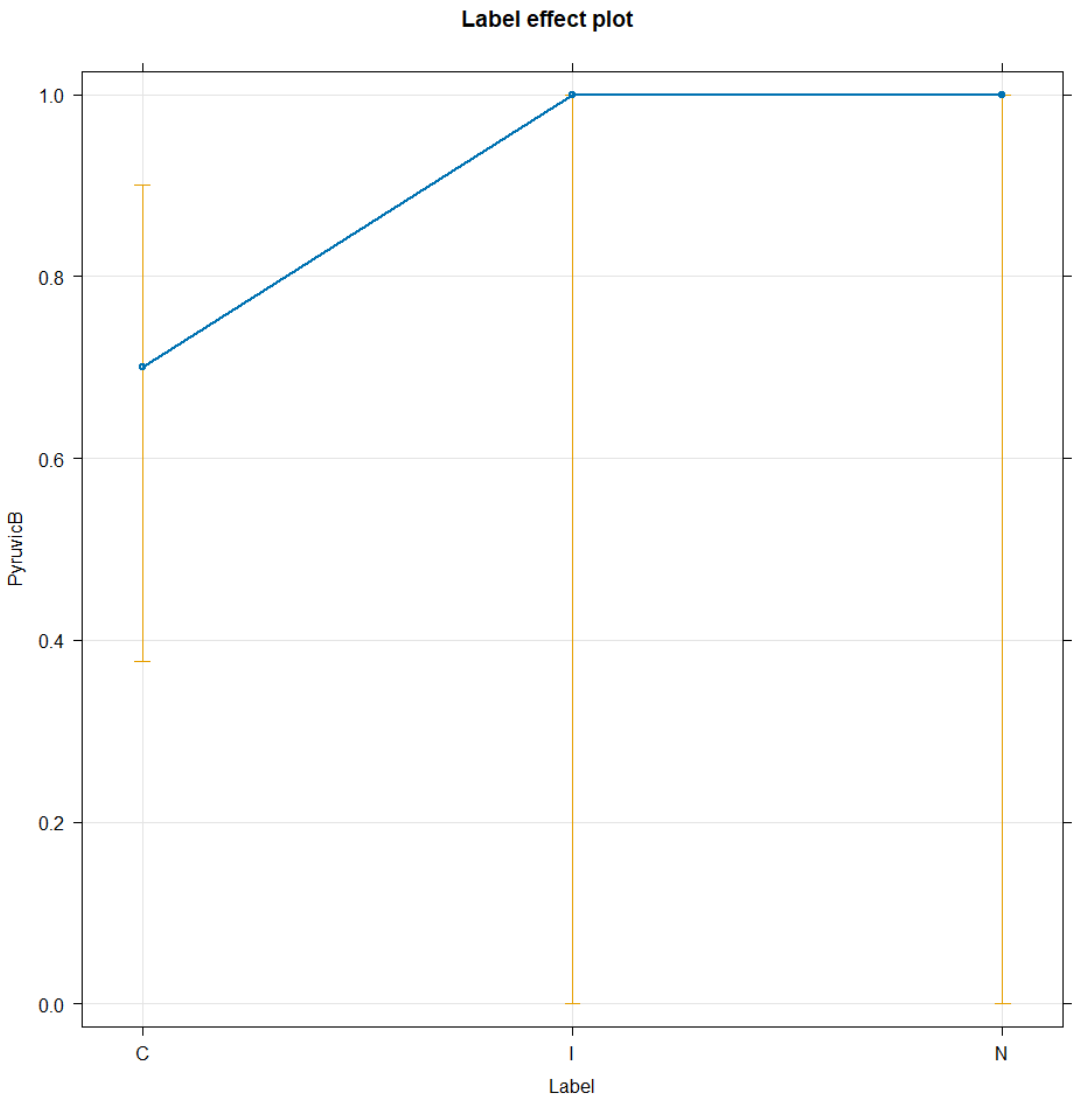
Label effect plot
1.0
0.8
0.6
0.4
0.2
0.0
PyruvicB
C
I
N
Label

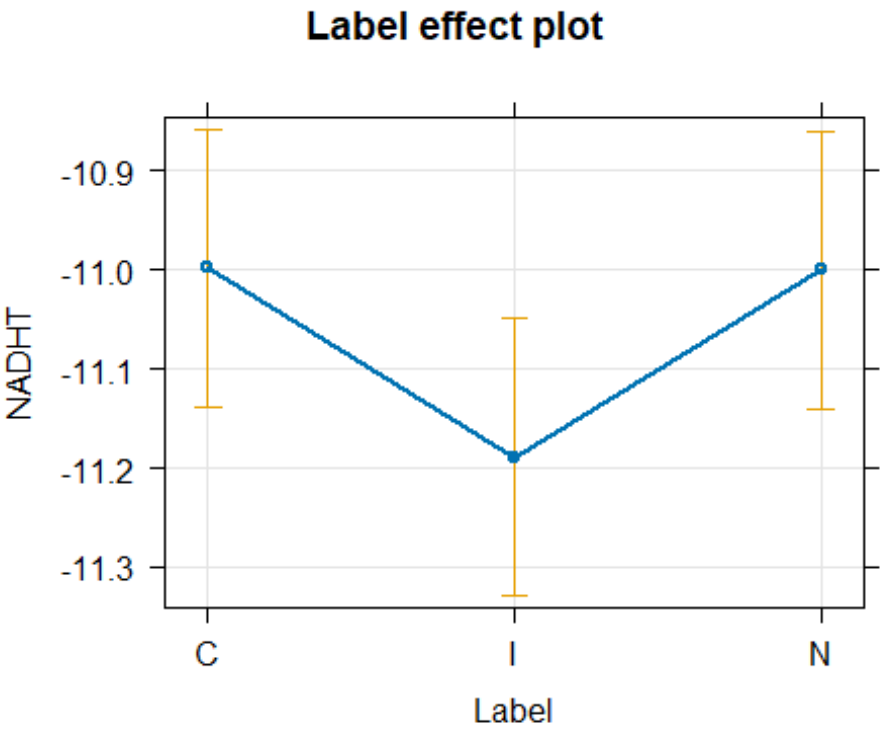
Label effect plot
NADHT
-10.9
-11.0
-11.1
-11.2
-11.3
C
I
N
Label

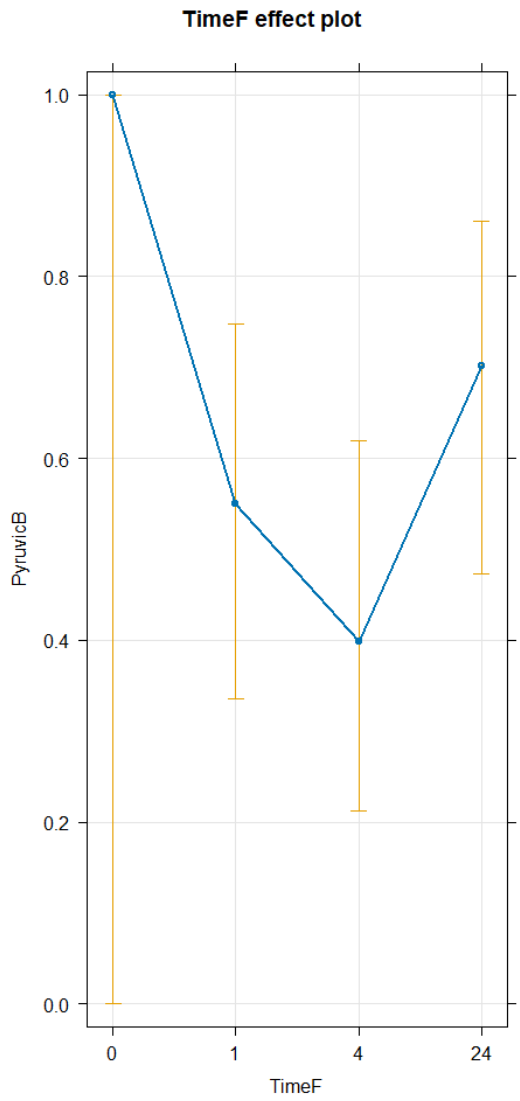
TimeF effect plot
PyruvicB
1.0
0.8
0.6
0.4
0.2
0.0
0
1
4
24
TimeF

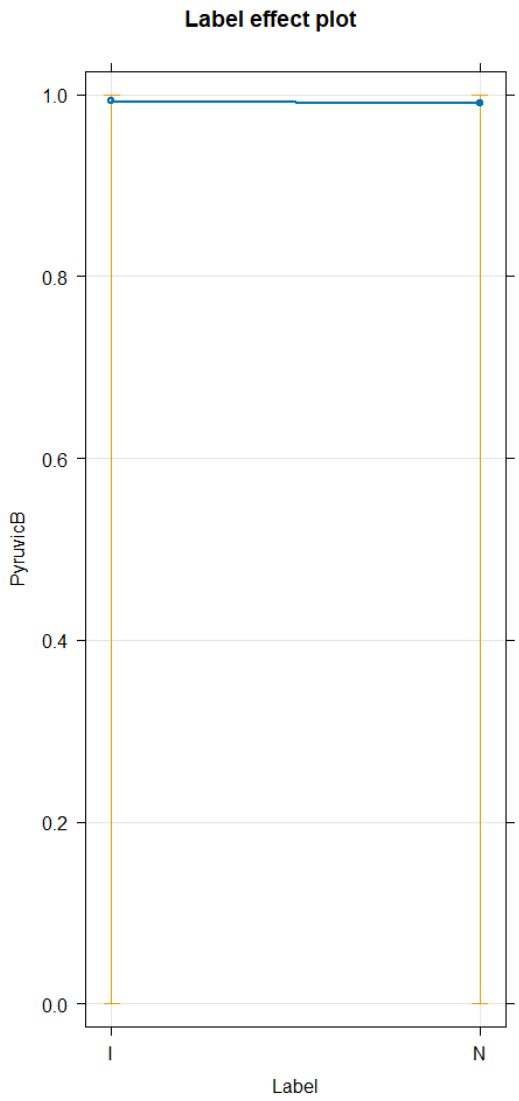
Label effect plot
PyruvicB
1.0
0.8
0.6
0.4
0.2
0.0
I
N
Label

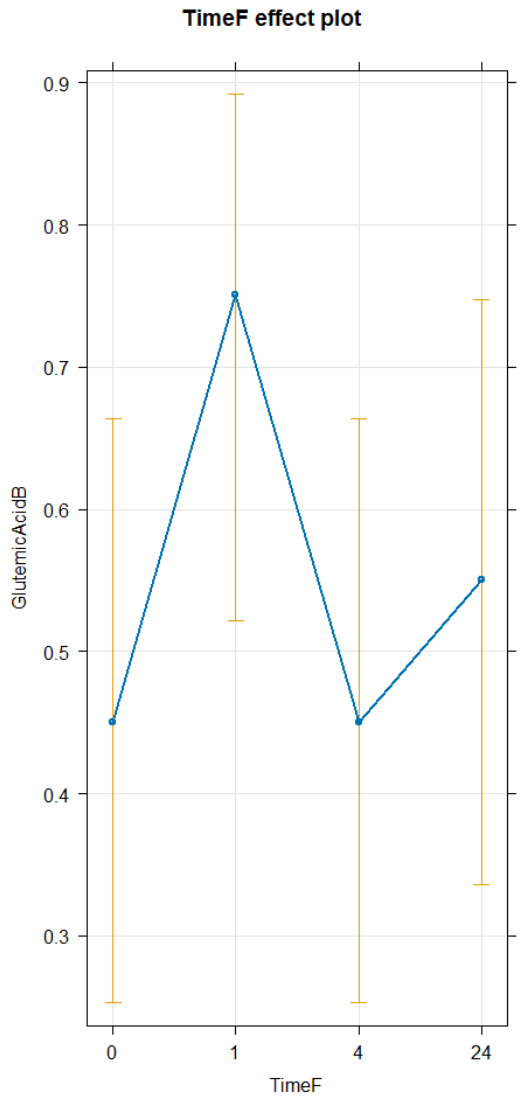
TimeF effect plot
GlutemicAcidB
0.9
0.8
0.7
0.6
0.5
0.4
0.3
0
1
4
24
TimeF

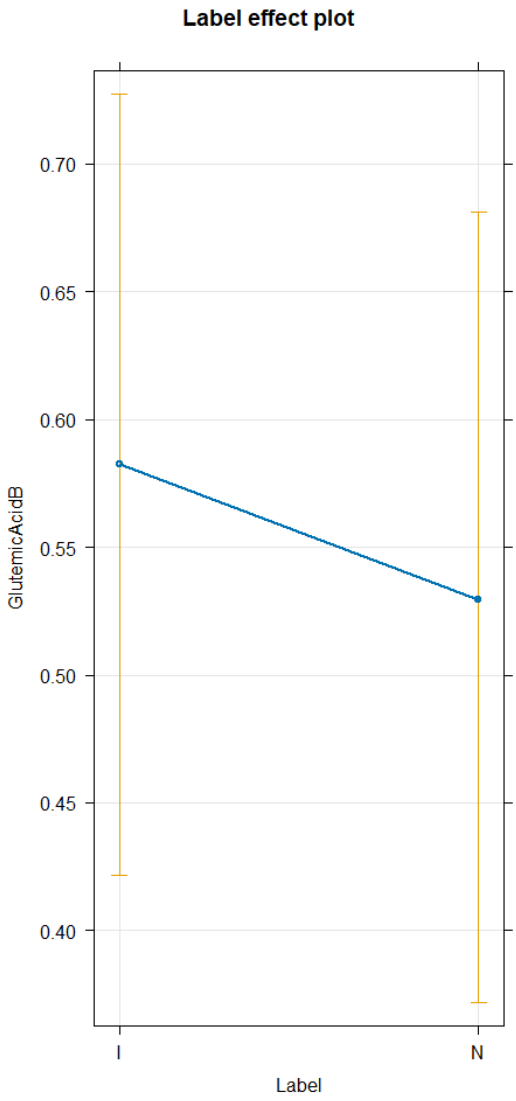
Label effect plot
GlutemicAcidB
0.70
0.65
0.60
0.55
0.50
0.45
0.40
I
N
Label

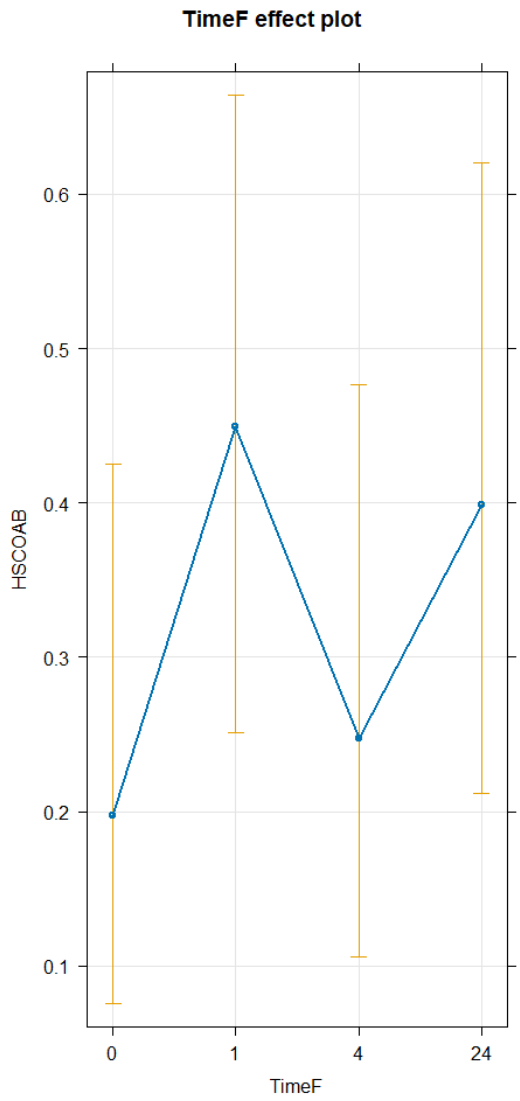
TimeF effect plot
HSCOAB
0.1
0.2
0.3
0.4
0.5
0.6
0
1
4
24
TimeF

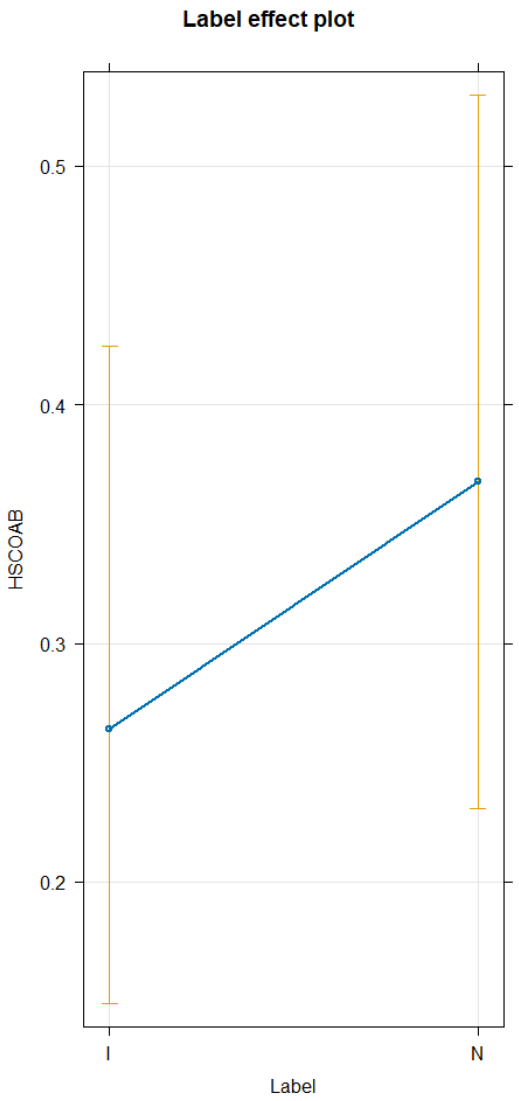
Label effect plot
HSCOAB
0.2
0.3
0.4
0.5
I
N
Label

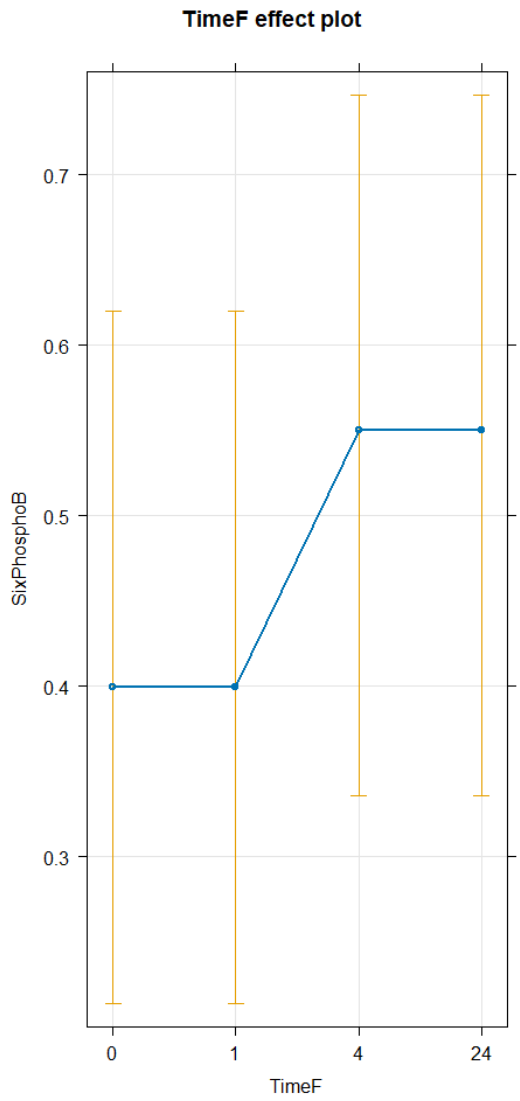
TimeF effect plot
SixPhosphoB
0.7
0.6
0.5
0.4
0.3
0
1
4
24
TimeF

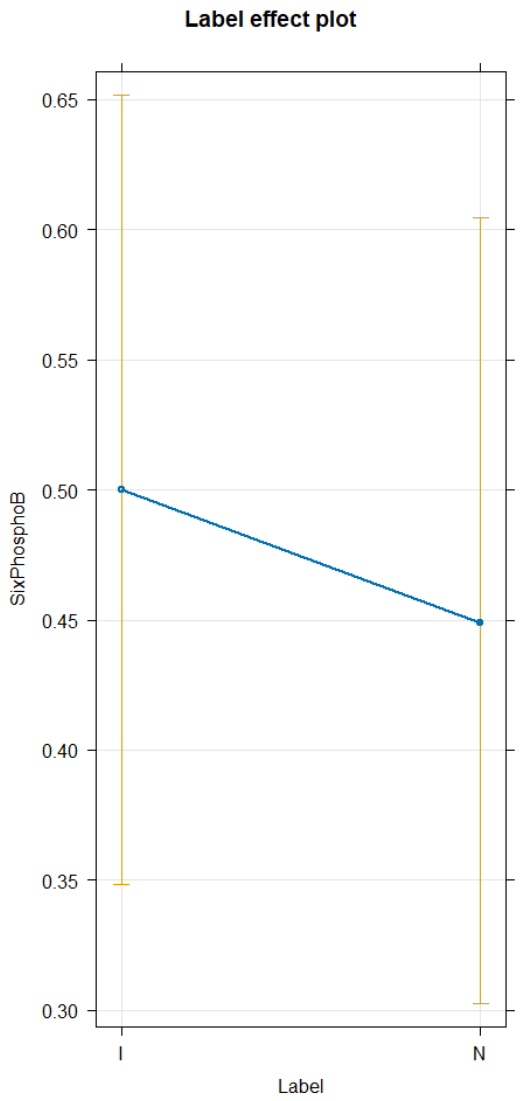
Label effect plot
SixPhosphoB
0.65
0.60
0.55
0.50
0.45
0.40
0.35
0.30
I
N
Label

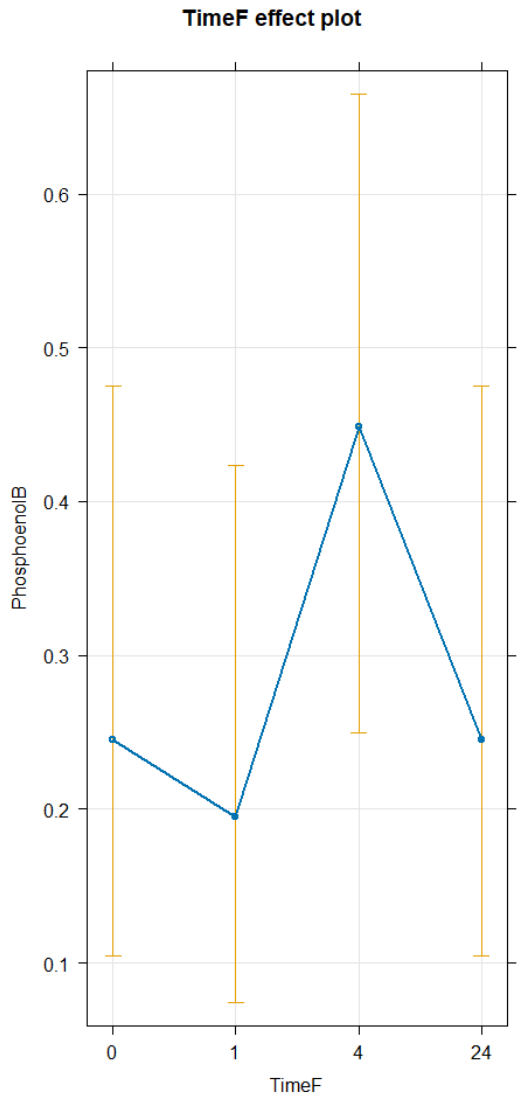
TimeF effect plot
PhosphoenolB
0.6
0.5
0.4
0.3
0.2
0.1
0
1
4
24
TimeF

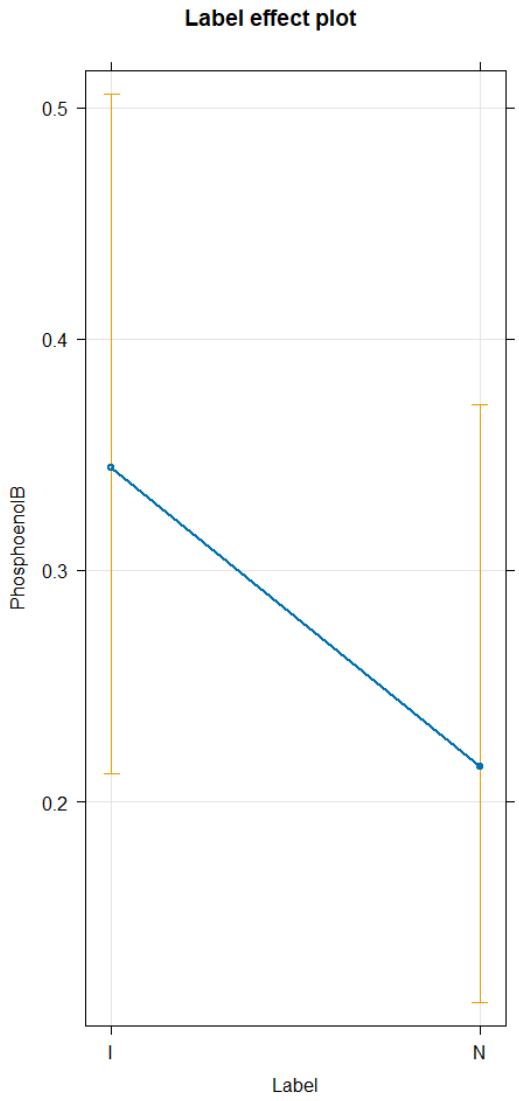
Label effect plot
PhosphoenolB
0.5
0.4
0.3
0.2
I
N
Label